Escola de Camins
Escola Tècnica Superior d'Enginyeria de Camins, Canals i Ports
UPC BARCELONATECH

TESI DE MÀSTER

Màster

Civil Engineering

Títol

Robustness to corrosion of post-tensioned concrete slab bridges

Autor

Christelle Grange

Tutor

Joan Ramon Casas

Speciality

Structural engineering

Date

08.05.2015

Acknowledgments

It is important to me to thank in a global way the Polytechnic University of Catalonia and all of the associated members of staff for hosting me and for making my studies more and more attractive during my semester abroad as part of the Erasmus program. Thanks to their welcoming, guidance, support and availability, I remain more and more motivated and passionate by my studies in the Civil Engineering department. This master thesis was again the proof of such a support and concern from them.

I am grateful to in particularly two persons, for many reasons, which help me to make this thesis achievable.

First, I address many thanks to my supervisor, Professor Joan Ramon Casas, which gave me the opportunity to deal with a subject that I could chose, by personal interest. He also allows me making this thesis feasible by providing me many advises and information needed to compose with my subject. Most of all, I would like to thank him for his important support, his continuous help, his guidance and for his outstanding availability at many times.

Professor Joan Ramon Casas could introduce me to Giorgio Anitori (PhD at UPC) who was a considerable help for me when dealing with the software I had to use whose I didn't know anything about. I would like to thank him for his remarkable availability and his precious advises and guidance towards my study.

It is a pleasure to show gratitude to both of them, because they mainly maintain me more and more motivated, invested and interested into this thesis.

Abstract

This master thesis aims to quantify the robustness of post tensioned bridge and to study the effect of corrosion on tendons. A post tensioned bridge has been first design. Concrete with medium compressive strength and steel strands are combined to form the post-tensioned model which provides a very strong and good work structure.

The robustness is defined as the structural property that measures the degree of remaining structural performance after the structure has been damaged by corrosion. Corrosion is an electrochemical process which occurs under oxygen and moisture exposure. Many researches have been oriented toward the effect of corrosion on steel bars and toward the consequence on the robustness of the structure. As corrosion leads to reduction of steel area, the robustness of the structure is affected. Indeed, a loss of steel leads to a reduction of strength of the structure. Many definitions of robustness are available but very few practical proposals of a target of threshold value that defines the limit between what is robustness or not do exist. In the past 30 years, different researchers attempted to quantify the robustness. A new approach adequate to structures under deterioration has been used for this case study of a post tensioned bridge affected by corrosion. This approach consists of a robustness indicator $I_{R,D}$ which can be expressed by the area below the curve that defines the normalised structural performance f(D) as a function of the normalised damage D. The higher the robustness index, the more robust the structure is.

Through grillage analysis aided by software SAP2000, three damage scenarios have been compared. First, a loss of prestressed area due to corrosion has been applied on the first three most external tendons, secondly on the three middle tendons and finally an equivalent loss of steel area on all the tendons. The index of robustness $I_{R,D}$ have been calculated in function of the damage D for each cases. It has been noticed that the index of robustness is the highest when the corrosion affects uniformly the structure whereas the lowest index of robustness appears when the corrosion affects the first three tendons. This is due to the distribution of loads on the structure that has a clear two dimensional behaviour: the highest loads are applied at the edge of the structure therefore a loss of prestress area at this location has more effect on the robustness of the structure. However, the robustness indicator of each case is closed to each other _less than 1.5% difference. It

can be deduced that the robustness aspect of this type of bridge is not really affected by the corrosion and its reaction is little.

The corrosion is an environmental factor that affects the most the robustness aspect of a structure under high loadings rather than an uniform corrosion on the entire structure; but corrosion does not reduce considerably the robustness of a post tensioned slab bridge with massive cross-section.

Contents

List of figures

List of tables

0. Introduction

0.1. Context of this thesis

In the early part of the 20th century, Eugène Freyssinet, a French engineer applied the technique of prestressing concrete, using high strength steel which contributed to the success of the technique. This form of construction has led to building long span bridges and proved an important economical way of building durable bridges. Two types of prestressed bridge do exist: pre-tensioned and post-tensioned. Post tensioned bridge is the type of bridge which will be studied is this thesis. Post tensioned bridge consists of tendons made of steel strands to assure the structural performance of the bridge. Eurocode and several reviews state the design procedure of this type of structure, however, the robustness aspect of post tensioned bridges has been very few exposed since.

The robustness is the ability of a structure to withstand events, as corrosion. Robustness aspect has been several times qualified in the past 50 years and also quantified _Frangopol and Curley (1987); Biondini and Restelli (2008), Starossek and Haberland (2011); Lind (1995); Goshn and Moses (1998), Baker et al. (2008)_ by different measures systems _deterministic, probabilistic and risk. However, Starossek and Haberland (2011) concluded that it is difficult to adequate robustness with all the different structure types. Most of the measures link the damage system and intact structure under deterioration, such as corrosion.

As a consequence, a new objective was set: establish a robustness indicator which could be used to quantify the loss of resistance under different deterioration scenarios and exposures. Eduardo Soares Ribeiro Gomes Cavaco computed the idea of the ratio of several structural performance indicators on the intact and on the damage state of the structure. He related the robustness with the structural indicators of a structure. Hence, this time the structural criterion of the structure is used to quantify the robustness. It takes into account the fact that the structure can tolerate damage wherever it occurs on the structure, on a single member of spread all over the structure. Eduardo Soares Ribeiro Gomes Cavaco defined a robustness index $I_{R,D}$ including both the structural performance and the damage of the structure. This robustness index is expressed as the area below the curve that defines the normalised performance f(D) as a function of the normalised damage D. The index runs

from 0 to 1, 0 being the worth robust indicator and 1 a full robust performance. The idea in this thesis is to use this robustness index to quantify the robustness aspect of a simply supported post tensioned bridge, by using corrosion as the damage on tendons. Corrosion is an electrochemical process under oxygen and moisture exposure. It affects a lot steel and reduces its area; therefore it decreases also the structural performance of a structure. The aim of this thesis is therefore to study the robustness aspect of a post tensioned bridge affected by corrosion at different levels of damage and to quantify it.

0.2. Aims and objectives:

To do so, the following objectives will be reached:

- The first step is to get familiar with the post tensioned concept and the design of a post tensioned bridge. A simply supported bridge will be design following Eurocode guidelines as a support for the analysis.
- The use of a computer aided method for analysis of bridge decks will help to compute different deterioration scenarios. Hence, one of the aims of this thesis is to know how to compute different models on the software SAP2000. SAP2000 is a finite element analysis software which is convenient for designing, modelling, displaying and analysing structures. An equivalent grillage will represent the bridge deck and allows its analysis. This is the grillage model analysis method. Building the grillage, understand how it works and in what way it is similar to the post tensioned bridge will also be a challenge.
- The last objective of this thesis is to use the robustness index under different corrosion situations and compare them to each other in order to determine which corrosion scenarios affects the most the structure. Moreover, the robustness criterion of a post tensioned bridge will be determined in order to establish if the corrosion can be withstand by this type of bridge.

0.3. Outline

The first part of this thesis will be dedicated at describing the post tensioning concept and its use in the construction. Following, a literature review will expose the robustness concept, its definition and its different way to qualify and quantify the robustness of different structures.

Secondly, a complete methodology of this thesis will be exposed, detailing and explaining how to achieve the objectives of this thesis.

Then, the design of a simply supported post tensioned bridge will be completed, by using Eurocode guidelines.

Afterward, the grillage analysis method will be exposed. By the use of the software SAP2000, the bridge will be modelled as an equivalent grillage in order to run a structural analysis.

Finally, the robustness index will be calculated under different corrosion scenarios and compared in order to determine its impact on the post tensioned bridge.

I. Post tensioned bridge concept

1. Prestressed concrete

Prestressed concrete is one of the most recent forms of construction related to structural engineering. High strength concrete and steel strands are combined to provide very strong and good work structures as roof slabs, bridges and railroad ties. In the early part of the 20th century, Eugène Freyssinet, a French engineer applied the technique of prestressing concrete, using high strength steel which contributed to the success of the technique. This technique has several uses in the construction field; the most widespread is to keep cables taut when subjected to compressive forces. The most familiar application is however the use in concrete when subjected to a prestressed force inducing an axial compression.

In bridge engineering, the introduction of the prestressed technique has led to the construction of long span bridges. Also, the use of prestressed concrete beams for smaller bridges, in particular for simply supported beams, has shown an economical form of bridge construction.

Many advantages of the use of prestressed concrete rather than reinforced concrete exist. The most important one is that for a given span and loading, prestressed concrete requires smaller members, which reduced the self-weight (dead loads in long span structures are the largest proportion of the total loads) and foundation costs. Moreover, suitable prestressing structures can be rendered crack free, which is an important factor for the durability of structures.

Prestressing offers also a way to control deflections. Usually, in the opposite direction of the load deflection, a vertical deflection is caused by a prestressed force eccentric to the centroid of a member. Therefore, by a suitable choice of prestress force, the deflections underneath applied load can be reduced or eliminated.

There are three concepts involved in the design of prestressed concrete:

- The first one transforms concrete into an elastic material. Concrete maybe treated such as for design at normal working loads. From this concept the criterion of no tensile stresses in the concrete was evolved. For simply supported beams, the bottom fibre

stress under dead load and prestress should be considered as the maximum allowable stress. Also, under dead loads, live loads and prestress the stress is considered to be the minimum allowable. Therefore under dead loads and prestress, as the dead loads moment reduces towards the support, then the prestress moment will have to reduce accordingly to avoid exceeding the permissible stresses.

- The second concept involved prestressing concrete to be considered as a combination of steel and concrete: the steel is taking tension and concrete compression so that the two materials form a resisting couple against the external moment. This concept is utilized to determine the ultimate strength of prestressed beams.
- The last concept involved using prestressing to achieve load balancing. In order to obtain a uniform compression of concrete, the tendons may produce an upward load which balances the downward load due to dead load.

2. Methods of prestressing

There are two methods of prestressing: pre-tensioning and post-tensioning.

a. Pretensioning

This method involved steel tendons that are tensioned between anchorages and the concrete members cast around the tendons. The steel tendons are in the form of wires or strands. Once the concrete has hardened sufficiently, the end anchorages are released and the prestress force is transferred to the concrete through the bond between the steel and concrete. The end of the tendons is then cut to produce the finish concrete member. As a large area of contact surface as possible is required, pretentioned members have usually a large number of wires or strands to provide the prestress force since the force in them is developed by bond to the surrounding concrete.

The use of in situ prestressing is widely developed in cable stayed and suspension bridge construction. In order to reduce the deflections of the bridge and also to optimize the deck cross section the stays are tensioned (Nawy, 1996).

For prestressed concrete bridge, the main used types of beams are:

- Inverted T-beams: usually used for spans between 7 and 16 metres, the voids between beams is fill with in situ concrete thus forming a solid deck.

- M-beams: usually used for spans between 14 and 30 metres, they have a thin slab cast in situ spanning between the top flanges. They form a voided slab deck. However, the access to the top flange is difficult which means that it is not possible to replace it. That's why Y beams have been introduced in 1990.
- Y-beams: they have been introduced to act as M beams but are easier to replace in case of damages. That also led to SY-beams which are used for spans between 32 and 40 metres.
- U-beams: usually used for spans between 14 and 34 metres where torsional strength is required.

b. Post tensioning

This method involves the pre-loading of the concrete which reduces the tensile stresses induced by the dead and live loads. In this case, the prestressed force is applied by jacking steel tendons against an already-cast concrete member. The tendons are threaded through ducts cast into the concrete.

Once the tendons have been fully tensioned the jacking force is transferred to the concrete through special built in mechanical anchorages. The force is usually provided by many individual wires or strands grouped into large tendons _general terms to define the high strength steel lengths used in post-tensioning_ and fixed to the same anchorage (figure 1).

Figure 1: bonded post tensioned beam with tendons in flat ducts

The live anchorage is the one at the jacking end whereas a dead anchorage is the one at the non-jacking end. Bond between the strand and the concrete is stopped by a tube through which the strand goes in order to allow the strand to stretch in the hardened concrete under the load applied by the jack. The tube is called a duct or sheathing, and is made of plastic or metal (figure 2) (Corven John, Moreton Alan, 2013-5; Bijan, 2000).

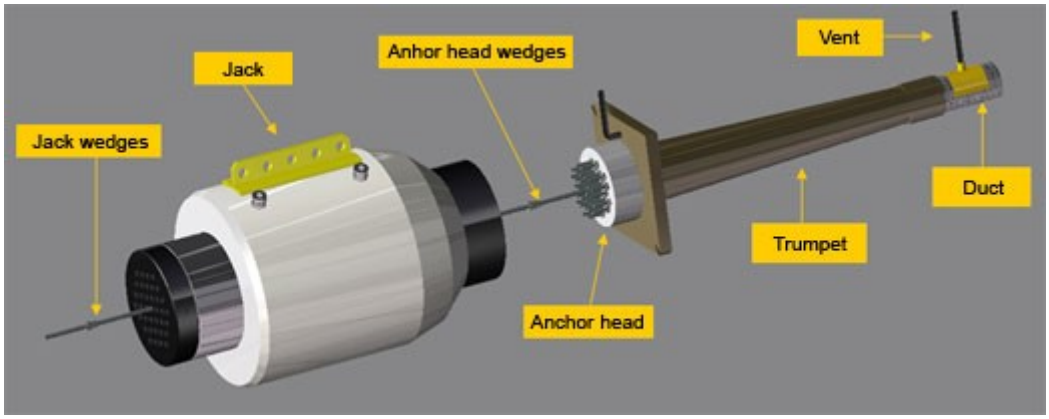

Figure 2: sketch showing the post tensioning procedure

After stressing the duck is grouted with cement mortar by the use of a mechanical pump (figure 3).

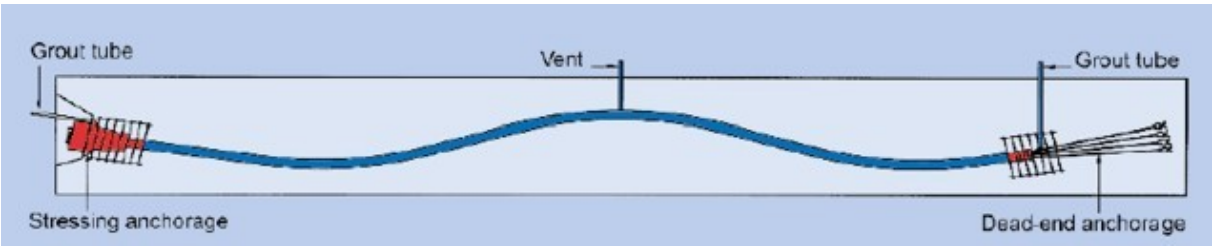

Figure 3: sketch showing the post tensioning principle

Post tensioning has become very popular for the past 50 years, since the technology has been perfected. First, there were problems with corrosion of the cables but better materials and construction methods have surely eliminated most of those problems.

Post tensioning allows the construction of special structures that would have been impossible to build, in particular due to site constraints or architectural requirements. It is also possible to use pre-cast concrete units which are post-tensioned together on site to form the bridge deck. Post-tensioning application are various, from offices and apartment buildings, to bridges and sports stadium. One of the most common applications is slabs on ground, where soils are expansive, unstable and likely to move. Moreover, post tensioning is used for strengthening existing structures such as an upgrade to resist seismic forces.

There are two post tensioning systems, classified as bonded or unbounded. Bonded system consists of filling the tendon ducts with mortar grout after stressing while unbounded involves greasing and paper wrapping, greasing and plastic covering or moisture tightening the tendons. Bonded systems are mainly used in bridges, in both superstructure and cable stayed bridges. This post tensioning system consists of tendons with multiple strands or bars. The most common form of tendons are 7 or 9 strands of 0.6" but a tendon can reach up to 19 strands (figure 4) (Andrew and Turner, 1991).

Figure 4: sketch showing a bonded system with 7 strands per tendon

3. Advantages of post-tensioning

Post tensioning is a technique that provides a lot of advantages at every stage of the construction and its uses over standard reinforcing steel.

One of the main advantages of this technique over pretensioning is that the tensioning is carried out in steps or stages, for all tendons in members. This is useful when the load is applied also in different stages.

Moreover, as it provides strong work, it allows:

- Smaller required quantity of concrete;
- Thinner slabs and other structural members;
- Reducing considerably costs.

Thanks to the post tensioning, it is now possible to design and build longer spans in elevated members, as beams of floors.

In a structural behaviour point of view, it reduces or eliminates shrinkage cracking thus there is no need of joints and fewer joints and cracks that do form are held tightly together.

Post tensioning also have the advantage to incorporate easily curved tendons. While the concrete is poured around the flexible ducts, they can be held to a curve shape (John P.Miller, 2012).

From an economical point of view, using post tensioning contribute directly to reduce considerably cost comparing to other methods of reinforcement due to:

- Less use of rebar;
- Less concrete demand;
- reducing material handling;
- Less labour needed or installation of material;
- Simplified formwork leads to less labour cost;
- Rapid re-use of formwork leads to less formwork on jobsite.

4. Stages of post-tensioning

Usually, the main stages of post-tensioning involve first the casting of concrete, then placing the tendons and afterward the anchorage block and jack. The tension to the tendons is then applied to finally seat of wedges (figure 5).

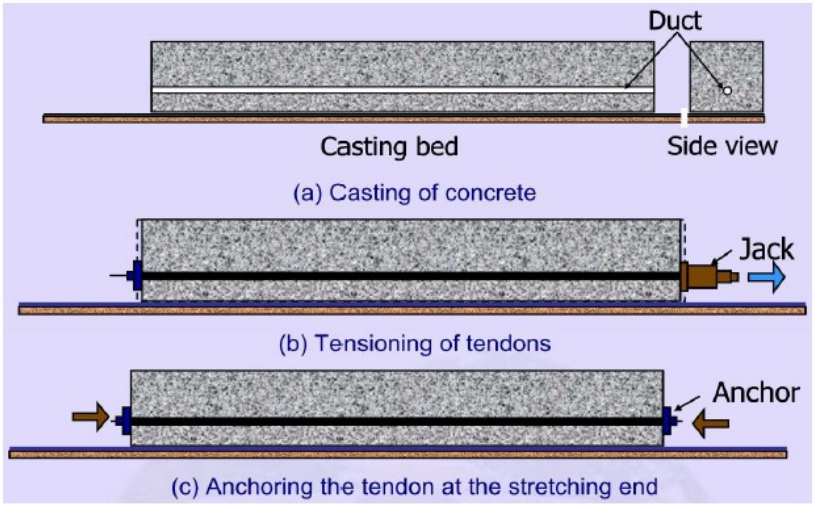

Figure 5: scheme showing the stages of post-tensioning (Dr. Amlan Sengupta and Prof. Menon, 2011)

5. Application of post-tensioning on bridges

As stated previously, post tensioning allows cost-effective construction of high-quality bridges, over a wide range of conditions and span lengths. This method offers high intrinsic durability and an ability to build bridges quickly with minimal impact on the human and natural environment. It also limits cracking, reduces structural depth and is ease of accommodating curved roadway alignment. All of those criteria benefits to building post-tensioned bridges (Post tensioning institute, 2000; VSL Report series, 1991)

.

The first post tensioned bridge ever built is in Oued Fodda, Algeria (figure 6). The idea came from Freyssinet and the bridge was erected by Campenon Bernard Company in 1936 and 1937. It consists of four anchorages with a total of twelve precast girders for a 20m span. The bridge still stands today.

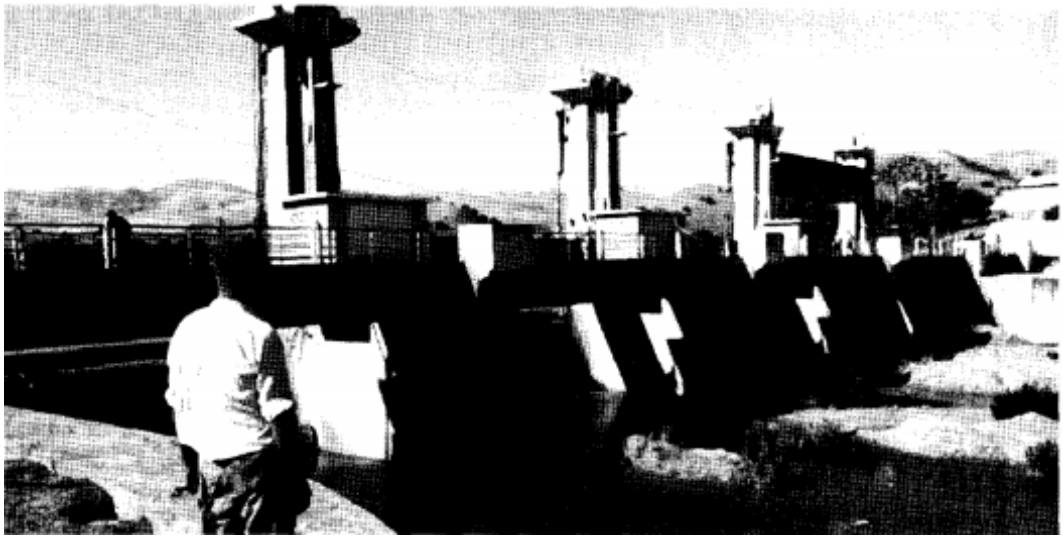

Figure 6: picture of the Oued Fodda Bridge (Algeria)

Post tensioning has been used to cross major bodies of water, deep mountain canyons and densely populated urban area as it allows long spans without touching the land or water below the bridge.

II. Robustness concept

1. Definition

The robustness concept in structural engineering is the ability of a structure (or part of it) to withstand events (like fire, explosion, and impact) or consequences or human errors, without being damaged to an extent disproportionate to the original cause (*ISO 22111*). In other words, robustness is defined as the structural property that measures the degree of remaining structural performance after the structure has been damage. Robustness is often incorporated to redundancy, but those two terms are different. Indeed, a structure is redundant if one particular component failure does not have any destructive influence on the remaining structure. Moreover, robustness is also linked to other terms, such as vulnerability, hazard, errors and consequences. Figure 7 displays the robustness and its related terms (Fink et Al, 2009).

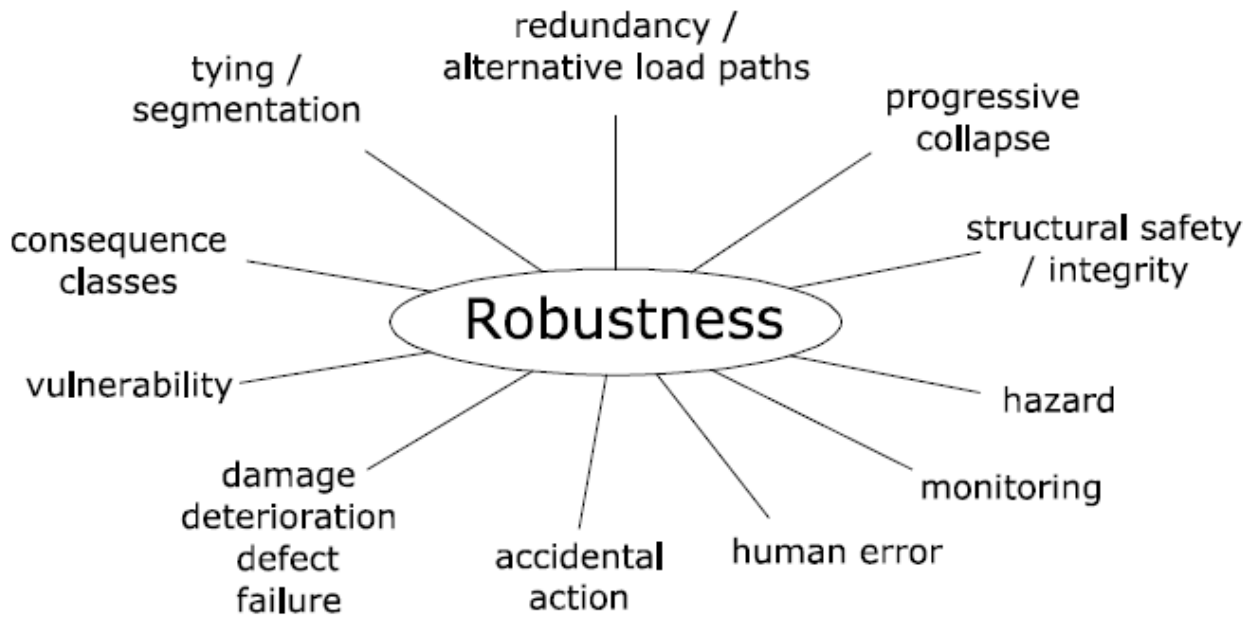

Figure 7: illustration of robustness and related terms (Fink, Steiger and Kohler, 2009)

The robustness of a structure is mentioned either from a structural property issue or from its environmental exposure (fire, hazard and other accidental actions). Both include damage and function losses, but environmental actions lead to consequences independent of structural properties. Therefore, robustness does not depend only on the structure only. From the event to the consequences, the robustness scheme can be summarized as follow (figure 8):

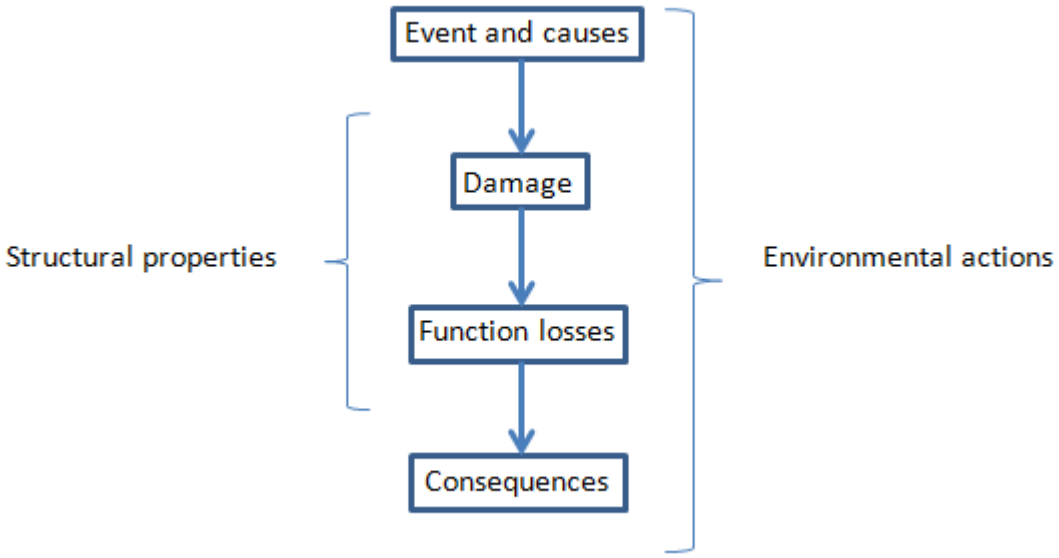

Figure 8: Robustness scheme comparing structural properties versus environmental actions (Eduardo Cavaco et Al, 2011)

2. Robustness measures

In order to compare one structural solution to another in term of robustness, three methods do exist. They help to define if one structural solution is more or less than another but they give only a relative value of robustness, which means that they do not provide a criterion to determine acceptable levels of robustness of a structure. Many definitions of robustness are available but very few practical proposals of a target of threshold value that defines the limit between what is robustness or not do exist. In the past 30 years, different researchers attempted to quantify the robustness.

Three main measures are distinct: deterministic, probabilistic and risk measures, all studied by researchers from 1987 (Figure 9).

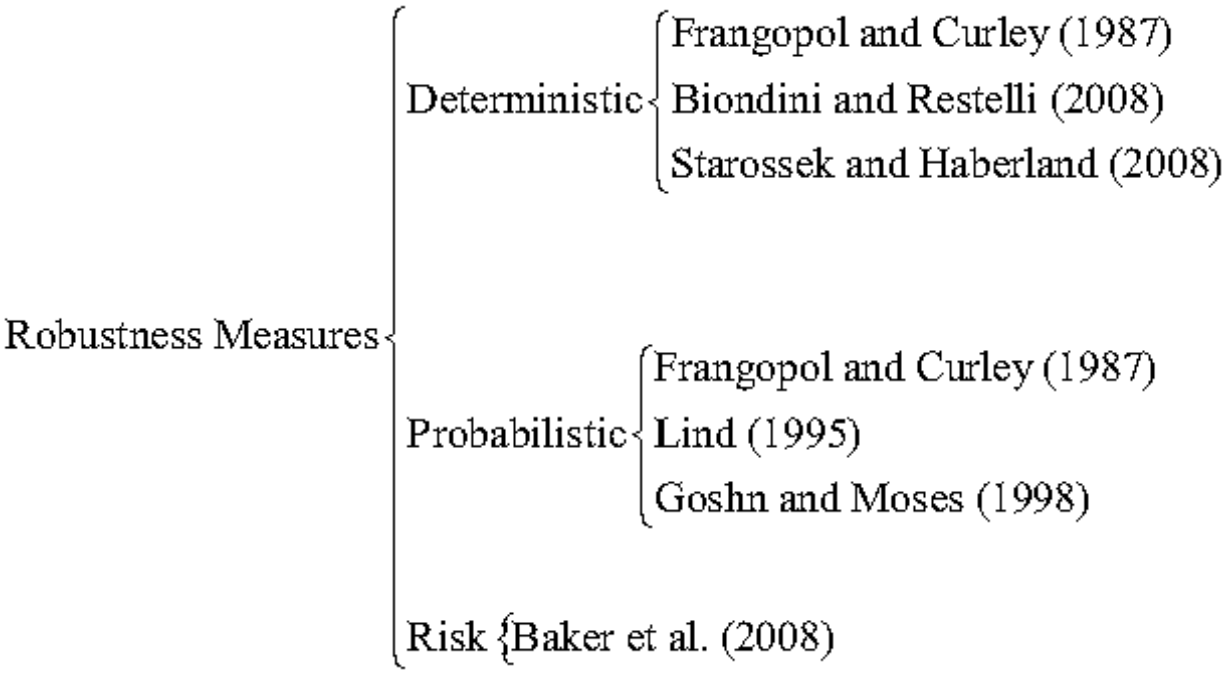

Figure 9: classification of robustness measures (Eduardo Cavaco et Al, 2008)

a. Deterministic measures

Deterministic measures allow providing a robustness indicator in function of the damage itself and its progression along the structure.

As discussed previously, robustness and redundancy are distinct parameters. Frangopol and Curley have suggested a deterministic indicator of redundancy, expressed in terms of the strength of the damage structure compared to the intact structure.

$R = L_{intact} / (L_{intact} - L_{damage})$

Where L_{intact} and L_{damage} represent the collapse loads of the structure without damage (intact structure) and considering damages respectively.

R is 1 if the structure has no reserve strength whereas R reaches an infinite value when the damage has no influence on the structure.

Ghosn and Moses expressed the robustness in function of three parameters. Two of them are about the intact configuration of the structure and the last one is calculated on a damages configuration.

Those three measures are

- $R_u = LF_u/LF_1$
- $R_f = LF_f/LF_1$
- $R_d = LF_d/LF_1$

Where LF_1 is the load causing failure of the first member;

LF_u is the collapse of the system;

LF_f is the functionality limit state and

LF_d is the collapse of the damage structure.

Finally, Starossek and Hoberland quantified robustness in function of the damage state. Three equations allow defining the robustness of a structure, at different stages of the damage progression. This includes:

- The damage progression caused by initial damage;

- The second damage-based measure in order to avoid the dependency of the first measure on the initial damage and

- The energy based measure based on energy released during collapse.

b. Probabilistic measures

Following their idea of expressing the redundancy by comparing the intact and the damaged criterion of a structure, Frangopol and Curley stated the redundancy index by estimating the probability of failure of the structure:

$$Ri = [P_{f\,(damaged)} - P_{f\,(intact)}] / P_{f\,(intact)}$$

Where $P_{f\,(damaged)}$ and $P_{f\,(intact)}$ are respectively the probability of failure of the intact system ad damaged system.

Lind also determined a probabilistic measure of the redundancy, mentioning the vulnerability of a system:

$$V = P(r_0,s) / P(r_d,s)$$

Where r_d is the resistance of the damaged system; r_o is the resistance of the intact system and S is the load. The value runs from 0 to infinite, a higher value provides higher impacts of damage on a system resistance.

c. Risk based measure

Risk-based measure is the most complete framework. The risk is expressed in function of different probabilities that characterise and modify the robustness of a structure:

$R = P(C/D) * P(D/E) * P€ * Cost(C)$

Where R is the risk;

P(C/D) is the collapse probability conditional on damage;

P(D/E) is the probability of damage to the exposure E;

P(E) is the probability of occurrence and

Cost(C) is the cost of collapse.

Based on risk of failure and collapse, Baker et Al suggested a robustness index which depends on the structure environment but cannot be considered as a structural property.

$$I_{robustness} = R_{dir} / (R_{dir} + R_{ind})$$

Where R_{dir} is the risks associated to the direct consequences of a local failure and

R_{ind} is the risks because of indirect consequences related to the collapse of the system.

3. Robustness index: a new approach

As stated by Starossek and Haberland (2011), developing a robustness measure that adequate different structures and collapse types is difficult. Different measures have been presented in the previous section linking the intact and the damaged system, but the objective is now to suggest a new approach adequate to structures under deterioration, such as corrosion. This approach consists of a robustness indicator which can be used to quantify the loss of resistance under different deterioration scenarios and exposures. Eduardo Soares Ribeiro Gomes Cavaco mentioned the idea of computing the ratio of several structural performance indicators on the intact and on the damage state of the structure. As robustness is related to structural property and is linked to the structural ability to tolerate damages, Eduardo Soares Ribeiro Gomes Cavaco suggested a new definition of robustness:

"Robustness is a structural property that measures the degree of structural performance remaining after the structure has been damaged" Eduardo Soares Ribeiro Gomes Cavaco, 2011.

However, this definition does not refer to the collapse potential. It takes into account the fact that the structure can tolerate damage wherever it occurs on the structure, on a single member or if the damage is spread all over the structure or part of it. Previously, researchers have been developing measures to express the progressive collapse, that's why this new approach dismisses the collapse. The robustness index includes both the structural performance and the damage of the structure in order to avoid a lack of sensitive of the robustness measure. Therefore, the robustness index $I_{R,D}$ can be expressed by the area below the curve that defines the normalised structural performance f(D) as a function of the normalised damage D:

$$I_{R,D} = \int f(D)dD$$

This index runs from 0 to 1 for a worthless and full robustness of the structure respectively. Figure 10 shows the normalised structural performance function of normalised damage. The area under the curve represents the robustness index $I_{R,D}$.

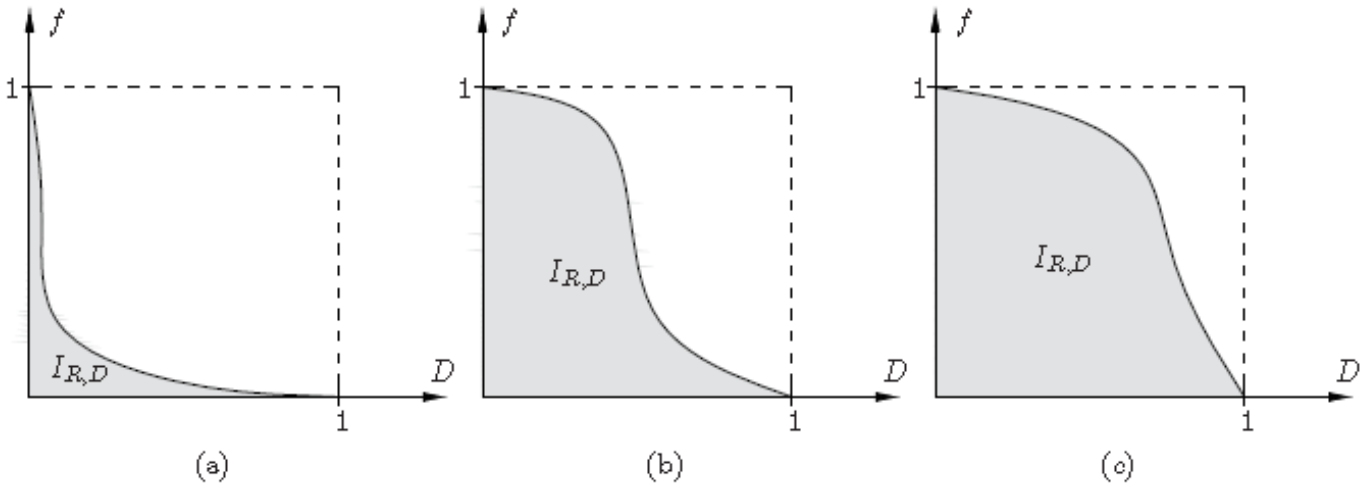

Figure 10: Graph showing the robustness index for (a) minimum robustness; (b) intermediate robustness and (c) maximum robustness

4. Robustness and corrosion

Corrosion is an electrochemical process which occurs under oxygen and moisture exposure. In absence of water or oxygen, the process does not occur. Many researches have been oriented toward the effect of corrosion on the cross section of steel bars by Thoft-

Christensen and Hansen (1994) and Darmawan (2010). Basically, oxygen, water and iron react to produce rust, the steel is oxidised which leads to a reduction in area and a reduction of strength of the steel.

$Fe + 3\ O_2 + 2\ H_2O = 2Fe2O_3H_2O$

⇔ (Steel) + (Oxygen) + (Water) = Hydrated ferric oxide (Rust)

The rate of corrosion on steel depends on many factors, but the most influent one is the surrounding environment of the structure: the climate, the proximity of the structure to water bodies and seawater exposition. As corrosion leads to reduction of steel area (Eyre et Al, 2000), the robustness of the structure is affected. Indeed, a loss of steel leads to a reduction of strength of the structure. The corrosion is an environmental action as explained on figure 11.

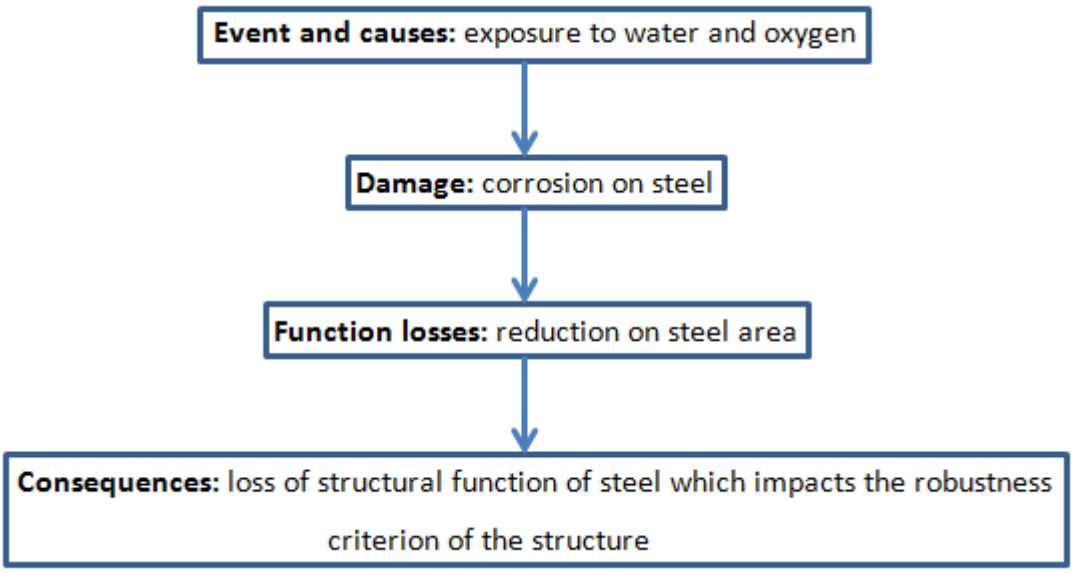

Figure 11: Robustness scheme applied to corrosion action

III. Methodology

As stated in the introduction, the aim of this thesis is to compare the robustness of a post tensioned bridge affected by corrosion on tendons at different locations of the bridge cross section.

Therefore, in order to achieve this goal, preparations stages including the design of the bridge are needed. The main stages are:

- The first main stage is the design of post-tensioned bridge by using the Euro codes. This includes determining the loadings, the characteristics of the structure and its design.
- From the design recommendations, the required area of prestressed reinforcement will be determined. The bridge will be tensioned by tendons comprising nine strands forming a certain area of prestressed. Thus, the number of tendons required can be calculated and the final design of the bridge is obtained.
- The bridge will be then modelled as an equivalent grillage in order to run its analysis by using the method of "grillage analysis" developed by Hernnikoff and Absi. Grillage Analysis is a computer aided method for analysis of bridges decks, by the use of the software SAP2000.
- Once the grillage will be sharped and its member's properties will be defined, loads will be applied on members. Running the analysis will be then possible, under different load combinations in order to obtain moments and reactions at support. This will allow verifying the model by checking its similarity to the bridge.
- From the results, it is then possible to calculate the stress distribution along the bridge span. The stress depends on the moments exerted by variable, dead and prestressed loads; it also depends on the inertia of members and on the distance between the centre of gravity and the top or bottom of the section for respectively the stress at the top and at the bottom of the section.
- As the moment exerted by the prestressed force is related to the stress, it is possible to calculate different values of stresses in function of different prestressed loads. The corrosion affecting the tendons leads to a loss of prestressed area, therefore to a loss of prestressed load. In this manner, it is possible to include the effect of the corrosion

on the structural assessment of the bridge. Thus, the robustness will be expressed through a load factor: a factor linking the stress exerted by the prestressed load and the robustness index.

Three different scenarios will be studied (Figure 12):

a) A loss of prestressed area induced by the corrosion on the three outermost tendons on the left hand side of the structure;

b) A loss of prestressed area induced by the corrosion on the three tendons located at the centre of the structure and

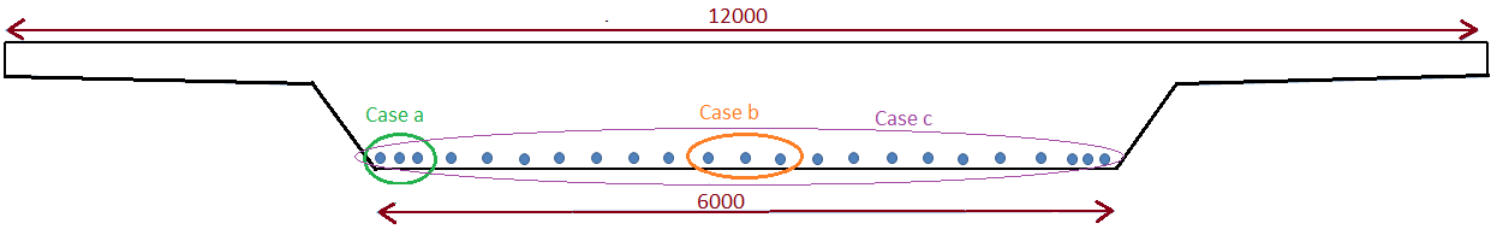

Figure 12: Sketch showing the different study cases

c) A loss of prestressed on all the tendons of the structure.

- As a result, three different index of robustness will be obtained. The aim of the thesis will be then achieved by comparing those indexes. The robustness of the bridge will be described for the three study cases; it will be then possible to find out where the corrosion affect the most the robustness criterion of the bridge.

IV. Design of a post tensioned concrete bridge deck

1. Basis of design/general information

The study case for this thesis consists of a simply supported post tensioned bridge. The span is 20 meters long and the width of the deck is 12m. The deck is made of concrete and prestressing strands from ASTM A-416 Standard are required. Barriers of type New Jersey barriers of 0.5m width and a surfacing of 8 cm have also to be taken into account. Appendix I shows the cross section of the deck.

2. Loadings

Unlike reinforced concrete design, the minimum load condition is always the most important one for concrete prestressed design. As the concrete section is a simply supported deck, the minimum bending moment at any section is the one which occurs immediately after transfer of the prestress force. This is often due to the self-weight of the deck. Soon after transfer the prestress concrete deck is moved from its framework. Therefore, it can be assumed that the prestress force is a maximum since only the short-term losses have occurred.

a. Permanent loads

Three loads are considered as permanent loads: the self-weight of the concrete bridge, the self-weight of the surfacing, and the self-weight of the barriers.

- Self-weight of the bridge:

Knowing that $\gamma_{concrete}$ = 25 kN/m^3, the self-weight of the concrete bridge is

$G_{concrete} = \gamma_{concrete} * Area = 25*8.175 =$ <u>204.375 kN/m</u>

- Self-weight of surfacing:

Knowing that $\gamma_{sufacing}$ = 24 kN/m^3, the self-weight of the surfacing is

$G_{surfacing} = \gamma_{surfacing} *$ width * thickness = 24 * 12 * 0.08 = <u>23.04 kN/m</u>

- Self-weight of the barriers:

Knowing that the weight of a New Jersey barrier is 1.57kg/m, the self-weight of the barriers is

$G_{barriers}$= 1.57 *2 = 3.14 kg/m = <u>0.03 kN/m</u>

Therefore, the total permanent load is equal to:

$G_{tot} = G_{concrete} + G_{surfacing} + G_{barriers}$ = <u>227.445kN/m</u>

b. Variable loads

Two traffic loads are considered as variable loads for this case study: the UDL system and the tandem system TS. Those two types of loads cover most of the effects of the traffic of lorries and cars. UDL are distributed loads while TS loads are punctual. The loadings are carried out by following recommendations from Eurocode 1 part 2 – Loads on Bridges.

Section 2.2 EN 1991-2:2003

The number and width of national lanes have to be defined first. The number of lane LN is calculated as follow:

N = w / 3m width per lane. The remaining width is called the Remaining Area. Knowing that the barriers take 2 *0.5m of carriageway, the number of lane is

N = (12-1)/3 = 3 LN + 2m of RA. This configuration (figure 13) is the equivalent configuration of the real carriageway (figure 14) when defining the loadings.

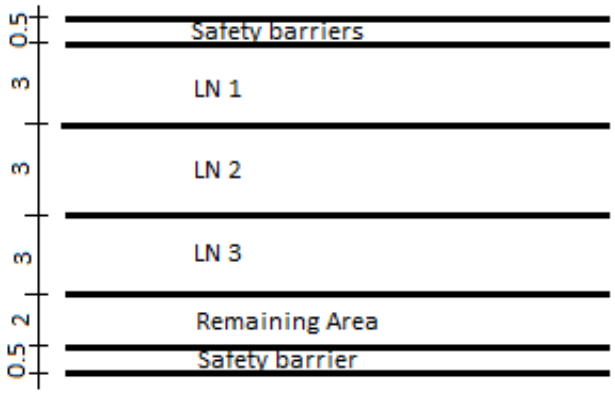

Figure 13: Equivalent configuration of the carriageway

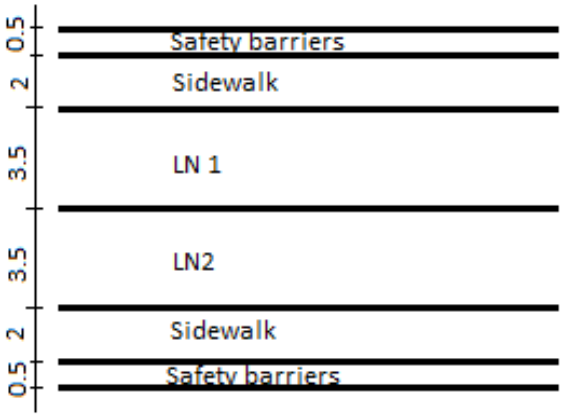

Figure 14: real configuration of the carriageway

From EN 1991-2:2003, the following characteristic values are applied (figure 15).

Location	Tandem system *TS*	*UDL* system
	Axle loads Q_{ik} (kN)	q_{ik} (or q_{ik}) (kN/m^2)
Lane Number 1	300	9
Lane Number 2	200	2,5
Lane Number 3	100	2,5
Remaining area (q_{rk})	0	2,5

Figure 15: Load Model 1, characteristic values (EN 1991-2:2003)

The details of the load model are illustrated in figure 16.

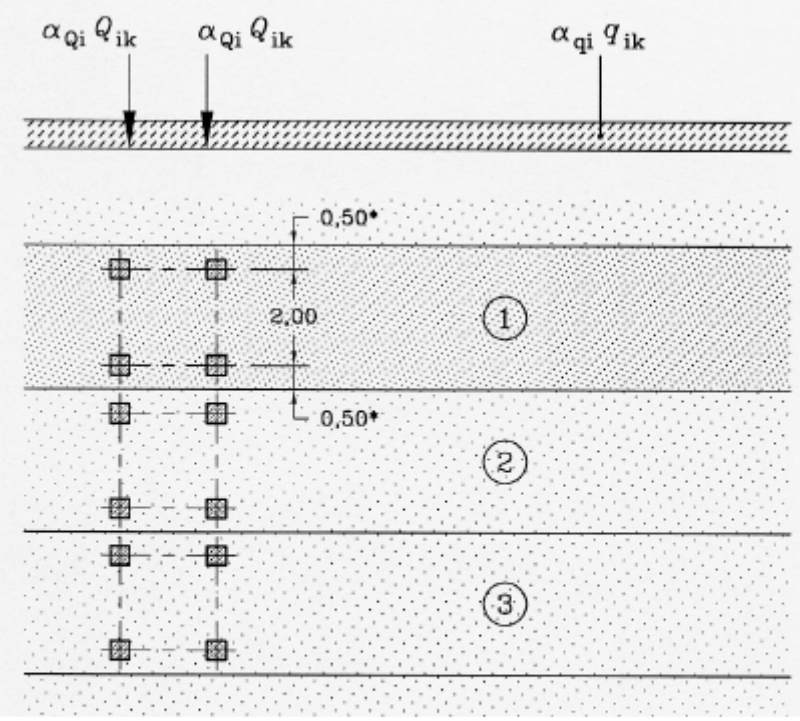

Key

(1) Lane Nr. 1 : $Q_{1k} = 300$ kN ; $q_{1k} = 9$ kN/m^2
(2) Lane Nr. 2 : $Q_{2k} = 200$ kN ; $q_{2k} = 2,5$ kN/m^2
(3) Lane Nr. 3 : $Q_{3k} = 100$ kN ; $q_{3k} = 2,5$ kN/m^2
* For $w_l = 3,00$ m

Figure 16: application of load model

Appendix II shows the variable loads on the bridge, their values and location.

3. Material properties

- Concrete properties *EN 1992-1-1*

The bridge has been designed for a design life of 50 years and exposed to moderate humidity or cyclic wet and dry exposure, which corresponds to a XC3 exposure class. The equivalent concrete is therefore RC 40, C32/40 (Table 4.1 EN1992-1-1:2004). Its properties are (Table 3.1 EN1992-1-1:2004):

- f_{ck} = 32 Mpa

- f_{cm} = 40 Mpa

- $E_{cm} = 22*(f_{cm}/10)^{0.3}$ = 33,35 kN/mm²

The nominal cover (Table 4.1 EN1992-1-1:2004) is 25mm+Δc where Δc=15mm therefore C_{nom}=25+15=40mm. The minimum cover is 40mm.

- Prestressing strands (according to ASTM A-416 Standard, table V)

The selected tendons for this case study consist of 9 strands of 0.6 inch diameter: 9/0.6". The associated weight of a tendon is 9.92 Kg/m for a section of 1 260 mm². The diameter is 63mm and the tendon capacity is f_{pu}=2 346 kN.

The required fabricated trumpet is CF-15 with the following dimensions (figure 17)(from Table VII, ATM A46-Standard):

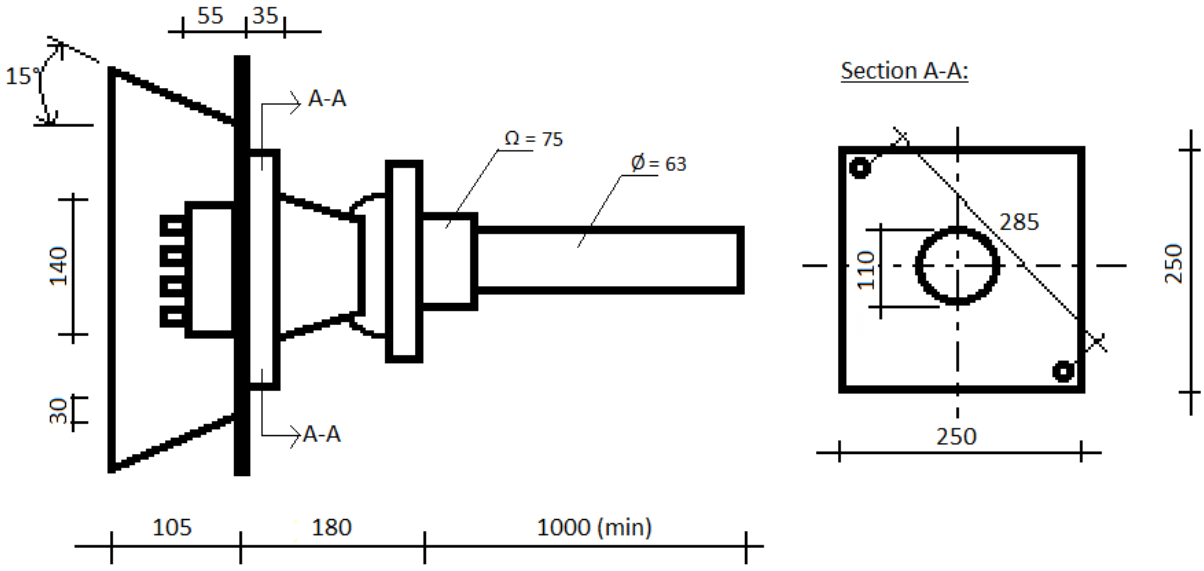

Figure 17: required trumpet and its dimensions for a 9/0.6" strand

- Properties of deck: area, centre of gravity and inertia of the bridge deck

The cross sectional area of the bridge deck and its inertia are calculated from the following table 1 with the help of figure 18, knowing that the inertia of a rectangle is $bh^3/12$ and the inertia of a triangle is $bh^3/36$:

Table 1: Table showing the calculation steps to obtain the properties of the deck

Bodies	Ai (m2)	yi	yi*Ai	Ii	di=yi-ybar	di2*Ai
1	3,0000	0,875	2,6250	0,01563	0,29980	0,26965
2	0,1250	0,716	0,0895	0,00007	0,14080	0,00248
2	0,1250	0,716	0,0895	0,00007	0,14080	0,00248
3	0,7000	0,700	0,4900	0,00058	0,12480	0,01090
4	3,9000	0,325	1,2675	0,13731	-0,25020	0,24413
5	0,1625	0,433	0,0704	0,00381	-0,14220	0,00329
5	0,1625	0,433	0,0704	0,00381	-0,14220	0,00329
Tot	**8,1750**	4,198	**4,7022**	**0,16129**	0,17163	**0,53621**

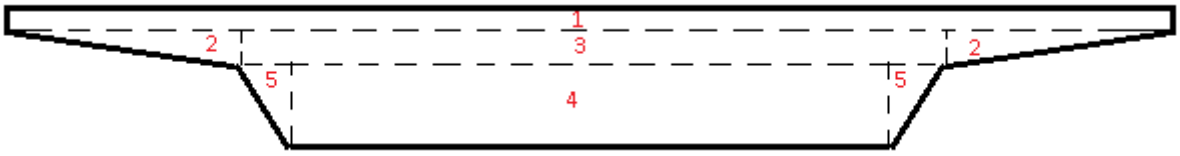

Figure 18: sketch showing the different bodies helping in the calculation of the properties of the deck

The total cross sectional area is 8.175 m². The centre of gravity can be first calculated:

$Y_{bar} = \Sigma(y_i * A_i)/\Sigma A_i = 4.7022/8.1750 = 0.575$m.

Then, the inertia is:

$I = \Sigma(I_i) + \Sigma (d_i^2 A_i) = 0.16129 + 0.53621 = 0.697499\ m^4 = 6.97499\ mm^4$.

Those three parameters (Table 2) will be useful for the design section.

Table 2: Summary of design parameters of the bridge deck

Area (m²)	8,175
Ybar (m)	0,575
I (m^4)	0,697499

4. Combination of actions

According to EN 1990, section 6 "Verification by the partial factor method", the combination of actions at Ultimate Limit State ULS and Serviceability Limit State SLS can be established.

- SLS

The frequent combination is the one recommended among the three load combinations (quasi-permanent; frequent and rare) as it represents a combination of sustained and variable imposed load. Indeed, it has a higher probability of being achieved and is used to check the limit state of cracking in prestressed concrete members.

The general format of effects using the frequent combination should be (*EN 1990, section 6.5.3, eq 6.15.a):*

$E_d = E\ (\Sigma \gamma_{Gj*} G_{kj} + \gamma_p * P + \psi_{1.1} * \gamma_Q * Q_k + \Sigma \psi_2 * Q_k)$

Annexe A, table A.2.1 defines the recommended values of ψ for road bridges (Table 3).

Table 3: recommended ψ values from Eurocode 1990

Traffic load gr1a:	ψ_0	ψ_1	ψ_2
TS	0,75	0,75	0
UDL	0,4	0,4	0

- For dead and surimposed dead loadings:

  $\Sigma G_k = 204.375 + 23.04 + 0.03 = 227.445$ kN/m

  Design SLS moment = $227.445 * 20^2/8 = 11\ 372.25$ kN.m

- For variable actions:

  - TS: $\Sigma Q_k = 1200$ kN

    Design SLS moment = 1200*20/4 = 6 000 kN.m

  - UDL: $\Sigma Q_k = 47$ kN/m

    Design ULS moment = $47 * 20^2/8 = 2\ 350$ kN.m

The combination of actions at SLS is:

$M_{SLS} = 11\ 372.25 + (0.75 * 6\ 000 + 0.4 * 2\ 350) =$ <u>16 812.25 kN.m</u>

- ULS

The general format of effects of actions should be *(EN 1990, section 6.4.3.2. eq 6.9.a)*

$E_d = E\ (\Sigma \gamma_{Gj} * G_{kj} + \gamma_p * P + \gamma_{Q1} * Q_{k1} + \Sigma \gamma_{Qi} * \psi_{Q1} * Q_{ki})$

Annexe A, table A.2.4 defines the partial safety factors (Table 4).

Table 4: partial safety factors from Eurocode 1990

	γ_{sup}	γ_{inf}
Dead loads	1,35	0,95
Surimposed dead loads	1,2	0,95
Traffic groups	1,35	0

- For dead and surimposed dead loadings:

  $\Sigma\gamma_G * G_k = 204.375*1.35+(23.04+0.03)*1.2 = 303.59$ kN/m

  Design ULS moment = $303.59 * 20^2/8 = 15\,179.50$ kN.m

- For variable actions:

  - TS: $\Sigma Q_k = 1200$ kN

    Design ULS moment = $1200 * 20/4 * 1.35 = 8\,100$ kN.m

  - UDL: $\Sigma Qk = 47$ kN/m

    Design ULS moment = $47 * 20^2/8 * 1.35 = 3\,172.5$ kN.m

The combination of actions at ULS is:

$M_{ULS} = 15\,179.50 + 8\,100 + 3\,172.50 =$ <u>26 452 kN.m</u>

5. Prestressed recommendations to Euro code 2

The prestressed force is applied to the concrete by prestressed tendons. The design of the deck and the prestressed tendons is completed according to eurocode 2. The effects of prestressing should be considered as a resistance or an action caused by prestrain and precurvature. Usually, prestress is introduced in the action combinations defined in EN 1990 as part of the loadings cases and its effects should be included in the applied internal moment and axial force. However, the contribution of the tendons to the resistance of the section should be limited to their additional strength beyond prestressing. The origin of the stress/strain relationship of the tendons is displaced by the effects of prestressing according to EN 1992-1-1:2004.

The following design of the deck is made by following *Eurocode 2 EN1992-1-1:2004*

- *Section 5-10-2-1*: Maximum stressing force

The maximum stressing force P_{max} applied to a tendon is expressed as

$P_{max}=A_p*\sigma_{p,max}$

Where $\sigma_{max}=\min\{k_1*f_{pk};k_2*f_{po,1k}\}$

With $K_1=0.8$ (recommended value)

$K_2=0.9$ (recommended value)

$F_{pk}=1900$ MPa

$F_{po,1k}=1700$ MPa (it is the characteristic 0.1% proff-stress of prestressing steel)

$\sigma_{pmax} = \min\{0.8*1900;0.9*1700\}$

$\sigma_{pmax} = \min\{1520;1530\}=1520$ Mpa

- *Section 5.10.2.2* : Limitation of the concrete stress

The concrete compressive strength should be limited to $\sigma_c<0.6*f_{ck(t)}$ where $f_{ck(t)}$ is the characteristic compressive strength of the concrete at time t when it is subjected to the prestressing force.

- *Section 5-10-3:* Prestressed force

In post tensioning the prestressed force of the tendon should be checked by measurements. The prestressed force at t=o is the force immediately after tensioning or transfer and is calculated as follow:

$P_{mo}=A_p*\sigma_{pmo}$

Where σ_{pmo} is the stress in the tendon at t=0 and $\sigma_{pmo}=\min\{k_7*f_{pk};k_8*f_{po,ik}\}$

where k_7 and k_8 are recommended value respectively equal to 0.75 and 0.85 so

$\sigma_{pmo}=\min\{1425;1445\} =1425$ MPa

- *Section 5-10-5*: Immediate losses of prestress for post tensioning

During the various stages considered during the design and during the prestressing process, allowing a loss of prestress force is needed when designing the deck. The value of 25% of loss of prestressed has been assuming for the calculation of the force.

6. Final design

Figure 19 shows the design notations in function of the prestressed force applied to the cross section of the bridge.

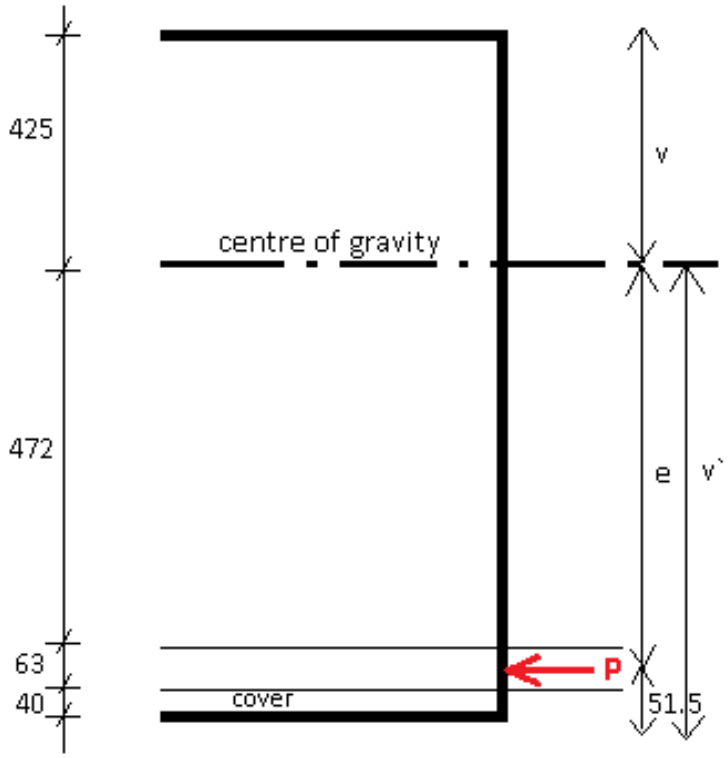

Figure 19: Cross section of the bridge and its design notation

The stress applied in the section is expressed as follow:

$\sigma_p = P_\infty/A + P_\infty*(e*v'/I)$

$= P_\infty/8\ 175\ 000 + P_\infty*(420.5*575/(6.97499*10^{11}))$

$= 4.6897*10^{-7}*P_\infty$ MPa

The stress loads is expressed as:

$\sigma_{loads} = M_d*v'/I$

Where M_d is the maximum design moment at serviceability as the design of prestressing is always done at the SLS rather than at the ULS for a concrete deck design.

$M_d = M_{SLS} = 17\ 124.75$ kNm

$\sigma_{loads} = 17\ 124.75*575/(6.97499*10^{11}) = 14.117$ MPa

As the stress at loading is equal to the stress σ_p, it is possible to sort out the prestressed force at t=∞:

$\sigma_{loads}=\sigma_p \Leftrightarrow$ 4.6897*10^-7*P_∞=17.117

$\Leftrightarrow P_\infty$=30 101 920.39 N

Due to the loss of prestressing of 25%, the prestressed force at t=0 is:

$P_0=P_\infty/(1-0.25)$=40 135 893.86 N

It is now able to calculate the area of prestressed: $A_p=P_o/\sigma_{pmo}$

A_p=40 135 893.86/1425=25 165.54 mm^2

The final required area of prestressed is 25 165.54mm^2.

Using 9 strands of 0.6´´ in one tendon, the area of prestressed in a tendon is

A_t=9*140=1260 mm^2

The number of tendons required is thus:

N = A_p/A_t = 28 165.54/1260 = 22.35 then 23 tendons are required in the deck.

The diameter of a tendon is 63 mm and the minimum spacing required is the maximum between the cover of 40mm and the diameter of a tendon (63mm) therefore the spacing between two tendons should not be less than 63mm.

The total space required to fit all of the tendons in the deck is taking into account the cover, the tendons and the spacing between:

- Cover=2*40mm=80mm
- Tendons=23*63mm=1449mm
- Spacing=22*63mm=1386mm

The total required space is 80+1449+1386=2 915mm. The bottom part of the deck is 6m wide so all of the tendons can fit in the deck. As the highest tandem loads are located near the edge of the deck and therefor are not above the prestressed tendons, It has been decided to input at each edge three tendons closed to each other with the minimum spacing required and then to distribute the other tendon in an uniform path along the deck.

Appendix III shows the prestressed tendons distribution.

V. Grillage model

Grillage Analysis is a computer aided method for analysis bridges decks. It came over when some authors, in particularly Hernnikoff, suggested a finite number of elementary frameworks modelling the continuous systems to study the elastic problems of a structure.

"The basic idea of the method consists in replacing the continuous material of the elastic body under investigation by a framework of bars, arranged according to a definite pattern whose elements are endowed with elastic properties suitable to the type of problem, in analysing the framework and in spreading the bar stresses over the tributary areas in order to obtained stresses in the original body. The framework so formed is given the same external outline and the boundary restraints, and is subjected to the same loads as the solid body, the loads being all applied at the joints" (Hrennikoff 1941).

This is the most popular method for bridge deck analysis because it is easy to comprehend, to use and has been proved to be accurate enough for a wide range of bridge types. It can be also applied to a wider range of structures, such as cellular decks, skew and curve bridges; and to every type of loading cases and conditions, temperature and pre-stress loads.

The deck is representing by an equivalent grillage of beams elements connected and restrained at their joints. The dispersed bending and torsion stiffnesses along the slab are concentrated in the nearest equivalent grillage beam. The slab's longitudinal stiffnesses are concentrated in the longitudinal beams whereas the transverse stiffnesses are concentrated in the transverse beams. Ideally, the beam stiffness should be such that when the slab and its equivalent grillage are subjected to identical loads, the two structures should deflect identically. Moreover, the moments, shear forces and torsions in any grillage beam should be equal to the resultants of the stresses on the cross section of the part of the slab the beam represents. These are ideal conditions and can be only approximatively verified due to the different characteristics of the two types of structure.

The grillage will be realised with the aid of the software SAP 2000.

SAP 2000 is a finite element program, used to model, design, display and analysis a structure. This software performs static or dynamic, linear or non-linear analysis of structural systems. The analysis procedure can be divided into three parts:

- Pre-processing
- Solving
- Post processing

SAP 2000 is frequently used by civil engineers for the conception and the analysis of bridges, edifices and dams etc… This software is used for reinforced structures, steel frameworks, and other construction materials and under every type of loadings: punctual, linear, surfacing…

Using the method of grillage analysis for a deck bridge requires essentially four steps to be followed in order to expect design responses, from the realisation of the grillage to the analysis:

1. Realising an idealisation of the deck geometry into an equivalent grillage
2. Defining the grillage member section properties that are the bending inertias of members and the torsion
3. Distributing loads to nodes of the grillage
4. Verification of the model
5. Interpretation of the results

1. Realising an idealisation of the deck geometry into an equivalent grillage

The grillage mesh depends on the geometry of the deck, but because of the high number of various shaped decks, it is difficult to set proper rules and precise guidelines to establish a grillage mesh. However, there are still certain rules that fit to every type of decks (Hambly, 1991):

- It is important to think and establish a grillage in function of how the designer wants the deck to behave and in function of the corresponding design. Therefore, the grillage beams should coincide with the lines of designed strength. This corresponds to place them parallel to prestress or component beams, along the edge of beams, or along the lines of strength over bearing.
- A longitudinal member should be placed at the centre of the deck; a transversal member should also be located in the centre of the span.
- Forces distribution is also important to consider. Each edge grillage member should be close to the resultant of the vertical shear flows at the edge of the deck, in order

to obtain prototype/grillage equivalence as precise as possible. For a solid slab deck, this is about 0.3 the depth from the edge.

- The total number of longitudinal members can run from 1 to 20. One member is allowed if the slab is narrow enough to consider its behaviour as a single beam whereas 20 members are allowed if the deck is very wide and the design is critical enough to permit expense and trouble.
- The spacing of transverse members should be small enough for small loads distributed along longitudinal members in order to be represented by a number of point loads with accuracy (spacing should be about a quarter of the effective span).
- The transverse and longitudinal members should be approximatively the same in order to permit statically distribution of loads.
- Transverse and longitudinal grillage members should be at right angles.

From those general rules, the following arrangements have been made in order to define an equivalent grillage modelling as best as possible the studied bridge:

- The 2-dimensions grillage is located at the centre of gravity of the deck. From this point, a rectangular cross section is assumed and its length (6.284m) determines the width of the grillage.
- The first and last nodes are taken at 0.3d from both sides of the assumed cross section.
- The width between two longitudinal members and two transversal members should be in the same order of magnitude: 1m width between two transversal members seemed coherent; therefore 9 longitudinal members are required with an adjacent width of 0.7855m. This configuration allows placing a member on each direction in the middle of the grillage.
- Nodes make a link between each transversal and longitudinal junction. However, 4 nodes need to be added to represent the supports where the vertical displacement is equal to zero. The location of the supports is 1 meter from the bottom edge of the bridge; therefore the location of each supports is 1.442m from the edge of the grillage, located on the two external transversal members (Appendixes IV and V).

2. Defining the grillage member section properties that are the bending inertias of members and the torsion

a. Bending inertia

The bending inertias of interior longitudinal and both interior and external transverse members are calculated as follow (Hambly, 1991):

$I=bd^3/12$ [/m]

This considers each member representing the deck width to midway to adjacent parallel members.

- For longitudinal members:

  - Internal members (from the 2nd to the 8th members):

  $I_{int-l}=I_{l2} = I_{l3} = I_{l4} = I_{l5} = I_{l6} = I_{l7} = I_{l8} = b*d^3/12$

  where b=0.7855m and d=1m therefore

  $I_{int-l} =0.7855*1^3/12 = 0.06546\ m^4$

- For transversal members:

  - Internal members (from the 2nd to the 20th members):

  $I_{int-t}=I_{t\ 2\ to\ 20} =b*d^3/12$

  where b=1m and d=1m therefore

  $I_{int-t} =1*1^3/12 = 0.08333\ m^4$

  - External members (1st and 21st):

  $I_{ext-t} = I_{t\ 1} = I_{t\ 21} = b*d^3/12$

  Where b=0.5m and d=1m

  $I_{ext-t} = 0.5*1^3/12 = 0.04167\ m^4$

- The bending inertia of external longitudinal members are calculated in function of the inertia of internal longitudinal members and of the total inertia of the structure:

  $I_{ext-l} = (I_{tot}-\Sigma I_{int-l})/2$

  Where $I_{tot} = 0.697499\ m^4$

And ΣI_{int} = 7*0.065456 = 0.45822 m^4

Therefore $I_{ext-l} = I_{l1} = I_{l9}$ = (0.697499-0.45822)/2 = 0.1196395 m^4.

b. Torsion

The torsion in members is calculated as follow:

$C=bd^3/6$ [/m]

- For longitudinal members:

  $C_l=1*1^3/6=0.1667$ per meter width of slab in member.

- For the first and last members:

  $C_{l1}=C_{l9}=0.1667$[/m] *(0.3+0.7855/2)[m]=0.1155

- For the other members:

  $C_{l2\ to\ 8}=0.1667$[/m] *0.7855[m]=0.1309

- For transversal members:

  $C_t=1*1^3/6=0.1667$ per meter length of slab in member.

- For the first and last members:

  $C_{t1}=C_{t21}=0.1667$[/m] *0.5[m]=0.08335

- For the other members:

  $C_{t2\ to\ 20}=0.1667$[/m] *1[m]=0.1667

The table 5 summaries the properties of members:

Table 5: table summarising the properties of grillage members

	Longitudinal members		Transversal members	
	External	Internal	External	Internal
	1st and 9th	2nd to 8th	1th and 21th	2nd to 20th
Bending inertias (m^4)	0,11964	0,06546	0,04170	0,08333
Torsion (m^4)	0,06547	0,13090	0,08335	0,04167

3. Distributing loads to nodes of the grillage

This step consists of the application of the tandems loads and uniform distributed loads from traffic on the grillage. Only traffic loads are considered when realising a grillage

analysis. This is explained by the fact that the dead loads will be applied on the whole grillage as they are distributed and will not help in finding responses at particular parts of the grillage. Indeed, dead loads will uniformly deform the grillage. Therefore there is no interest to apply them as it will increase load cases and possible mistakes knowing in advance they are useless for the analysis.

Only the punctual loads are applied on nodes, whereas the distributed loads are applied on longitudinal members. However, moments can be applied on both nodes and longitudinal members.

a. Attribution of tandem loads on the grillage

Tandem loads are punctual loads applied on each lane on the road. There are divided in 12 distributed loads (see section II.2.b Variable loads), disposed as following (figure 20):

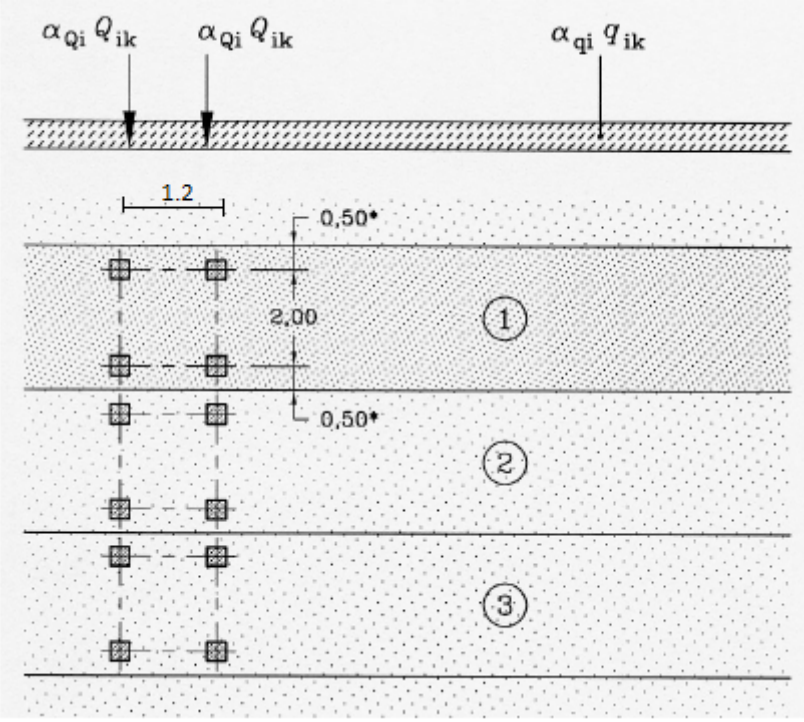

Figure 20: Sketch showing the distribution of tandem loads on the bridge

On the grillage, the associated location is shown on Appendix VI.

There are two ways of attributing loads on the grillage. Either it is possible to create new members linking the load to the closest member as show on figure 21 or it is possible to input them in function of their coordinates.

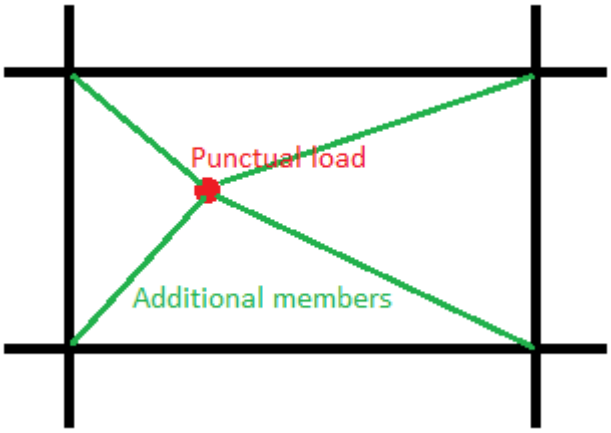

Figure 21: sketch showing how to create new members and attributing corresponding loads

The second option has been chosen for each type of loads. From their coordinates (figure 22), it is possible to find the associated load on each node (Table 6).

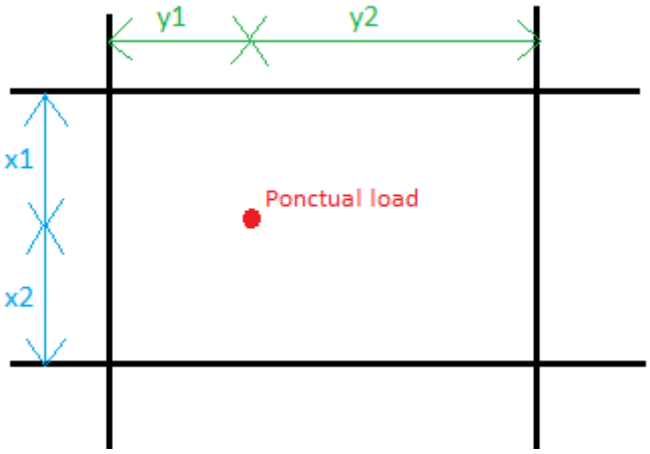

Figure 22: sketch showing the notation of coordinates helping in the calculation of equivalent loads on nodes

Table 6: table showing the calculation steps of tandem loads on nodes

	Load name	LN1a		LN1b		LN2a		LN2b		LN3a		LN3c	
	Load (kN)	150,000		150,000		100,000		100,000		50,000		50,000	
Coordi-nates of the load	Y (m)	0,786		0,786		0,786		0,786		0,786		0,786	
	y1 (m)	0,000		0,142		0,357		0,000		0,206		0,635	
	y2 (m)	0,786		0,643		0,429		0,786		0,580		0,151	
	X (m)	1,000		1,000		1,000		1,000		1,000		1,000	
	x1 (m)	0,600		0,600		0,600		0,600		0,600		0,600	
	x2 (m)	0,400		0,400		0,400		0,400		0,400		0,400	
Equivalent load on transversal members	on the 10th transversal member (kN)	90,000		90,000		60,000		60,000		30,000		30,000	
	on the 11th transversal member (kN)	60,000		60,000		40,000		40,000		20,000		20,000	
Equivalent load on nodes	**top-left (kN)**	**n 1-10**	**90,000**	**n 1-10**	**73,695**	**n 2-10**	**32,745**	**n 5-10**	**60,000**	**n 6-10**	**22,138**	**n 8-10**	**5,754**
	top-right (kN)	**n 2-10**	**0,000**	**n 2-10**	**16,305**	**n 3-10**	**27,255**	**n 6-10**	**0,000**	**n 7-10**	**7,862**	**n 9-10**	**24,246**
	bottom-left (kN)	**n 1-11**	**60,000**	**n 1-11**	**49,130**	**n 2-11**	**21,830**	**n 5-11**	**40,000**	**n 6-11**	**14,759**	**n 8-11**	**3,836**
	bottom right (kN)	**n 2-11**	**0,000**	**n 2-11**	**10,870**	**n 3-11**	**18,170**	**n 6-11**	**0,000**	**n 7-11**	**5,241**	**n 9-11**	**16,164**
Total equivalent load (kN):		150		150		100		100		50		50	

	Load name	LN1c		LN1d		LN2c		LN2d		LN3c		LN3d	
	Load (kN)	150,000		150,000		100,000		100,000		50,000		50,000	
Coordi-nates of the load	Y (m)	0,786		0,786		0,786		0,786		0,786		0,786	
	y1 (m)	0,000		0,142		0,357		0,000		0,206		0,635	
	y2 (m)	0,786		0,643		0,429		0,786		0,580		0,151	
	X (m)	1,000		1,000		1,000		1,000		1,000		1,000	
	x1 (m)	0,400		0,400		0,400		0,400		0,400		0,400	
	x2 (m)	0,600		0,600		0,600		0,600		0,600		0,600	
Equivalent load on transversal members	on the 11th transversal member (kN)	60,000		60,000		40,000		40,000		20,000		20,000	
	on the 12th transversal member (kN)	90,000		90,000		60,000		60,000		30,000		30,000	
Equivalent load on nodes	**top-left (kN)**	**n 1-11**	**60,000**	**n 1-11**	**49,130**	**n 2-11**	**21,830**	**n 5-11**	**40,000**	**n 6-11**	**14,759**	**n 8-11**	**3,836**
	top-right (kN)	**n 2-11**	**0,000**	**n 2-11**	**10,870**	**n 3-11**	**18,170**	**n 6-11**	**0,000**	**n 7-11**	**5,241**	**n 9-11**	**16,164**
	bottom-left (kN)	**n 1-12**	**90,000**	**n 1-12**	**73,695**	**n 2-12**	**32,745**	**n 5-12**	**60,000**	**n 6-12**	**22,138**	**n 8-12**	**5,754**
	bottom right (kN)	**n 2-12**	**0,000**	**n 2-12**	**16,305**	**n 3-12**	**27,255**	**n 6-12**	**0,000**	**n 7-12**	**7,862**	**n 9-12**	**24,246**
Total equivalent load (kN):		150		150		100		100		50		50	

The following figure 23 shows the notation of nodes, in order to obtain a better understanding of which nodes are concerned.

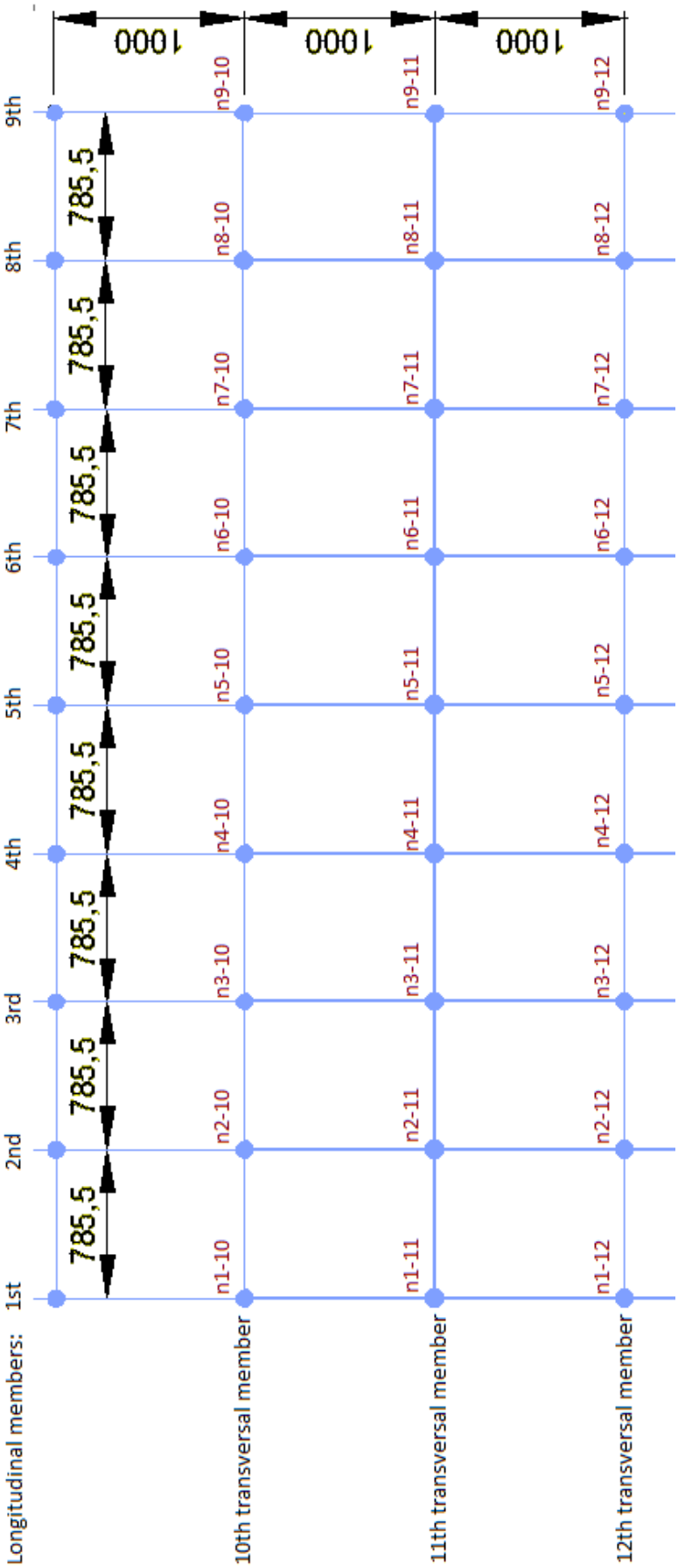

Figure 23: sketch showing the notation of nodes

The following table 7 shows the sum of loads on their corresponding nodes.

Table 7: attributed loads on nodes

Total equivalent load on nodes (kN):										
Longitudinal		1	2	3	4	5	6	7	8	9
Trans-versal	10	163,694853	49,050581	27,254567	0,000000	60,000000	22,138205	7,861795	5,753736	24,246264
	11	218,259804	65,400774	36,339422	0,000000	80,000000	29,517607	10,482393	7,671649	32,328351
	12	163,694853	49,050581	27,254567	0,000000	60,000000	22,138205	7,861795	5,753736	24,246264
									total:	**1200**

Moreover, the load LN1a and LN1c are not located on the grillage (1.85768m away on the left hand side), therefore the equivalent load is the combination of a punctual load and a moment. The punctual load has been attributed to the nodes as stated before, but the moment has been added to the first nodes on transversal members.

Calculation of moments on nodes:

$M_{n1\text{-}10}$=90*1.85768=167,1912 kN.m

$M_{n1\text{-}11}$=120*1.85768=222.9216 kN.m

$M_{n1\text{-}12}$=90*1.85768=167,1912 kN.m

Figure 24 shows the input of TS loads on the grillage model on SAP2000.

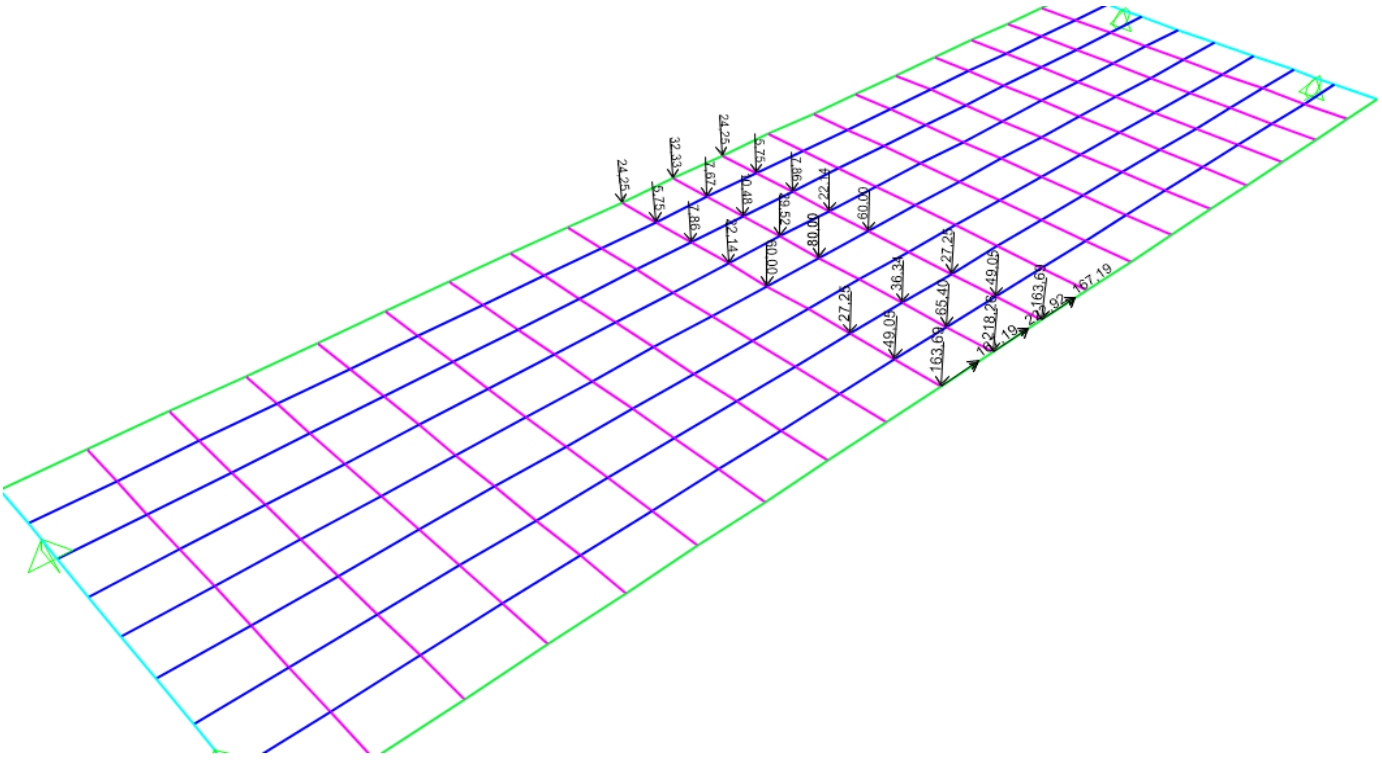

Figure 24: input of tandem loads on the grillage

b. Attribution of UDL loads due to traffic on the grillage

UDL loads due to traffic are distributed loads applied on each lane and on the remaining area (Appendix VII).

UDL loads due to traffic are disposed on longitudinal members only. They are calculated as follow: UDL (kN/m²) * width between two longitudinal members (m).

For the external members, the width is different than the one for internal members. Table 8 shows the calculation of the associated loads.

Table 8: table showing the calculation of associated loads on longitudinal members

UDL loads	
LN1 (kN/m²)	9
LN2 (kN/m²)	2,5
LN3 (kN/m²)	2,5
RA (kN/m²)	2,5

	Longitudinal members									
	l1	**l2**	**l3**	**l4**	**l5**	**l6**	**l7**	**l8**	**l9**	
Width (m)	2,7504423	0,7855	0,7855	0,7855	0,7855	0,7855	0,7855	0,7855	2,75106	Total
Equivalent load on members (kN/m)	**24,7540**	**3,5859**	**1,9638**	**1,9638**	**1,9638**	**1,9638**	**1,9638**	**1,9638**	**6,8777**	47,0000
equivalent moment on longitudinal members (kN.m)	**50,0415**	0,00	0,00	0,00	0,00	0,00	0,00	0,00	**13,9004**	63,9419

As shown in the table 8, there are two additional moments to consider on the external members _with a lever arm of 2.358m_ as UDL are distributed until the edge of the bridge, which represent a part that is not covered by the grillage.

Figure 25 shows the input of UDL on SAP2000.

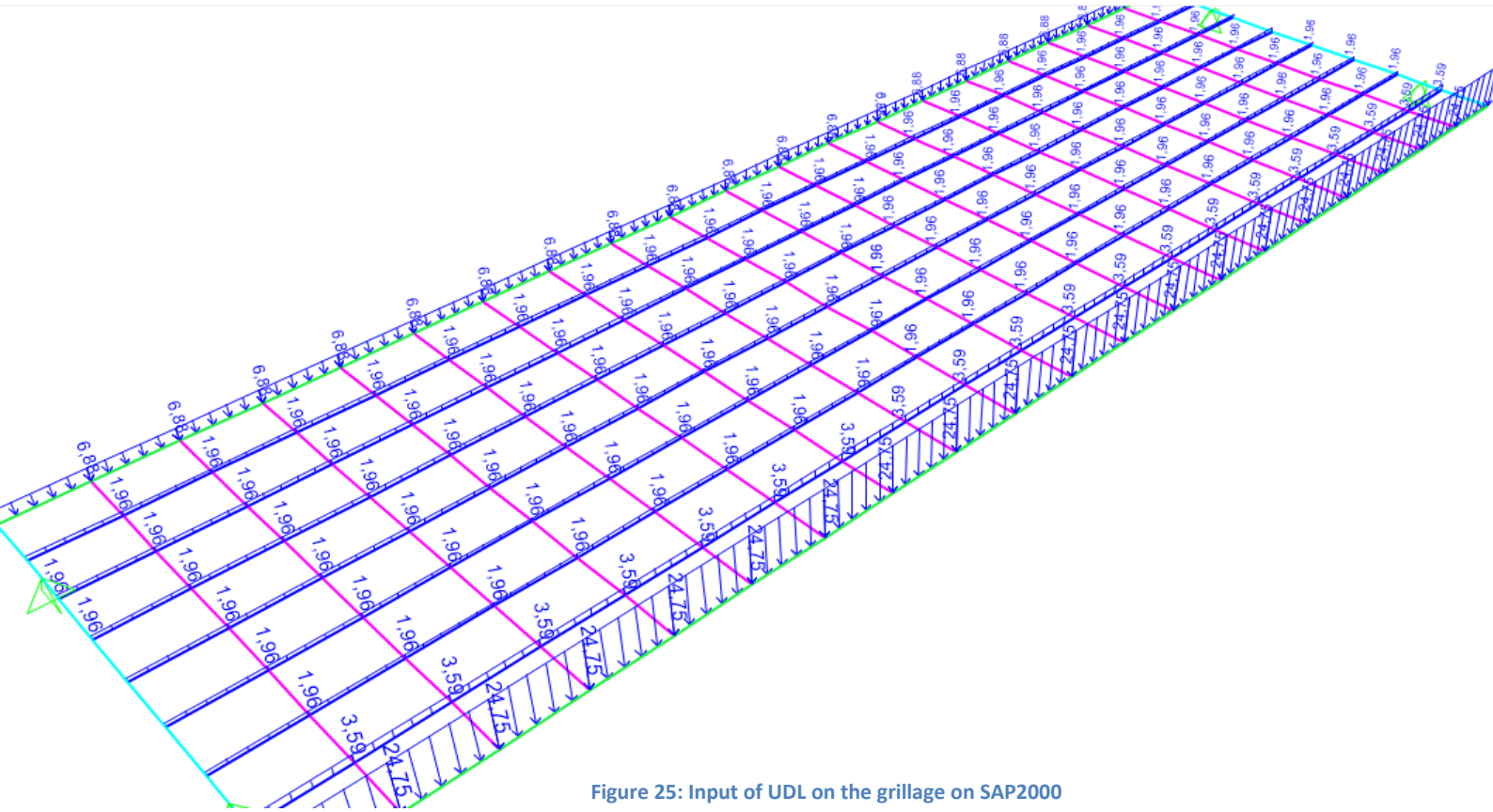

Figure 25: Input of UDL on the grillage on SAP2000

c. Prestressing load

The tendon exercises the prestressed force on the structure. The shape of the tendon is parabolic, and the two edges are anchored at the centre of gravity of the deck. The top of the tendon is located in the middle of the span (10m), with a distance to the centre of gravity equal to the eccentricity (Appendix VIII).

The prestressing force applied is in the uplift direction, as shown of the following sketch (figure 26):

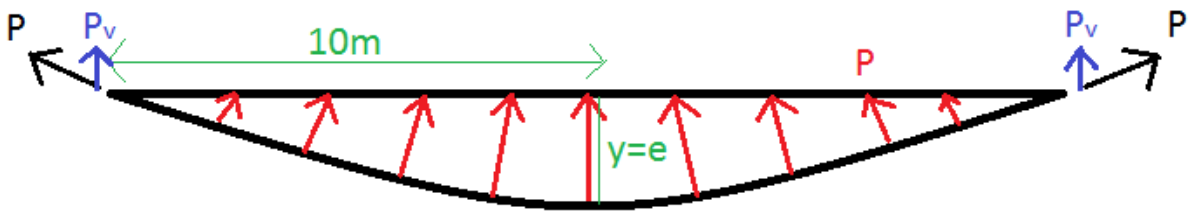

Figure 26: sketch showing the force of the prestressed tendons

The prestressed force induced by the tendon is a distributed load, equal to the prestressed force divided by the radius of curvature of the tendon:

$p = P / \delta$

where $P = P_0 = 40\,135{,}89386$ kN

The tendon has a parabolic shape whose equation is $y=ax^2+b$. As there is no eccentricity at the edges, b=0. Y is the eccentricity of the tendon at middle span where x = 10m (see figure 26 above). The radius of curvature is equal to the inverse of the second derivative of y:

$\delta = 1 / y''$

$= 1 / (ax^2+b)''$

$= 1 / (2a)$

Knowing that y = e = 420.5mm; x = 10m and b = 0, thus:

$a = y/x^2 = 0.4205/10^2=0.004205$

Therefore $\delta = 1/ (2* 0.004205) = 118.9$ m

Consequently, the prestressed force induced by a tendon is:

p = 40 135,89386 / 118.9 = 336.947 kN/m.

There are 23 tendons in the structure to cover the area of prestressed required (see section II.6 Final design) thus in one tendon the prestressed force is 336.947/23 = 14.6499 kN/m.

The force of the 23 tendons is represented by only 9 longitudinal members on the grillage; therefore the forces need to be distributed on the members in the same way as the UDL loadings (Table 9).

Table 9: table showing the distribution of the prestressed load of tendons on longitudinal members

	Prestressed member	1		2		3		4		5	
Coordinates of the load	Load	14,6499		14,6499		14,6499		14,6499		14,6499	
	Y (m)	0,7855		0,7855		0,7855		0,7855		0,7855	
	y1 (m)	0,2135		0,3395		0,4655		0,7629		0,2748	
	y2 (m)	0,572		0,446		0,32		0,0226		0,5107	
Equivalent load on longitudinal member	Left member (kN/m)	l1	10,66804	l1	8,318085	l1	5,968132	l1	0,421499	l2	9,524766
	Right member (kN/m)	l2	3,981863	l2	6,331815	l2	8,681768	l2	14,2284	l3	5,125134
	Total (kN/m)	14,6499		14,6499		14,6499		14,6499		14,6499	

	Prestressed member	6	7	8	9	10
Coordinates of the load	Load	14,6499	14,6499	14,6499	14,6499	14,6499
	Y (m)	0,7855	0,7855	0,7855	0,7855	0,7855
	y1 (m)	0,5722	0,0841	0,3814	0,6788	0,1907
	y2 (m)	0,2133	0,7014	0,4041	0,1067	0,5948
Equivalent load on longitudinal member	Left member (kN/m)	l2 3,978133	l3 13,0814	l3 7,536632	l3 1,989999	l4 11,09327
	Right member (kN/m)	l3 10,67177	l4 1,5685	l4 7,113268	l4 12,6599	l5 3,556634
	Total (kN/m)	14,6499	14,6499	14,6499	14,6499	14,6499

	Prestressed member	11	12	13	14	15
Coordinates of the load	Load	14,6499	14,6499	14,6499	14,6499	14,6499
	Y (m)	0,7855	0,7855	0,7855	0,7855	0,7855
	y1 (m)	0,4881	0	0,2974	0,5948	0,1067
	y2 (m)	0,2974	0,7855	0,4881	0,1907	0,6788
Equivalent load on longitudinal member	Left member (kN/m)	l4 5,546633	l5 14,6499	l5 9,103267	l5 3,556634	l6 12,6599
	Right member (kN/m)	l5 9,103267	l6 0	l6 5,546633	l6 11,09327	l7 1,989999
	Total (kN/m)	14,6499	14,6499	14,6499	14,6499	14,6499

	Prestressed member	16	17	18	19	20
Coordinates of the load	Load	14,6499	14,6499	14,6499	14,6499	14,6499
	Y (m)	0,7855	0,7855	0,7855	0,7855	0,7855
	y1 (m)	0,4041	0,7014	0,2133	0,5107	0,0226
	y2 (m)	0,3814	0,0841	0,5722	0,2748	0,7629
Equivalent load on longitudinal member	Left member (kN/m)	l6 7,113268	l6 1,5685	l7 10,67177	l7 5,125134	l8 14,2284
	Right member (kN/m)	l7 7,536632	l7 13,0814	l8 3,978133	l8 9,524766	l9 0,421499
	Total (kN/m)	14,6499	14,6499	14,6499	14,6499	14,6499

	Prestressed member	21	22	23
Coordinates of the load	Load	14,6499	14,6499	14,6499
	Y (m)	0,7855	0,7855	0,7855
	y1 (m)	0,32	0,446	0,572
	y2 (m)	0,4655	0,3395	0,2135
Equivalent load on longitudinal member	Left member (kN/m)	l8 8,681768	l8 6,331815	l8 3,981863
	Right member (kN/m)	l9 5,968132	l9 8,318085	l9 10,66804
	Total (kN/m)	14,6499	14,6499	14,6499

The final load on each member is shown on table 10.

Table 10: table showing the loads on each member

Total equivalent load on longitudinal members								
Longitudinal member	1	2	3	4	5	6	7	8
Equivalent load (kN/m)	25,37575	46,72675	38,40493	37,98157	39,96970	37,98157	38,40493	46,72675

Figure 27 shows the input of prestressed loads induced by the tendons on the grillage.

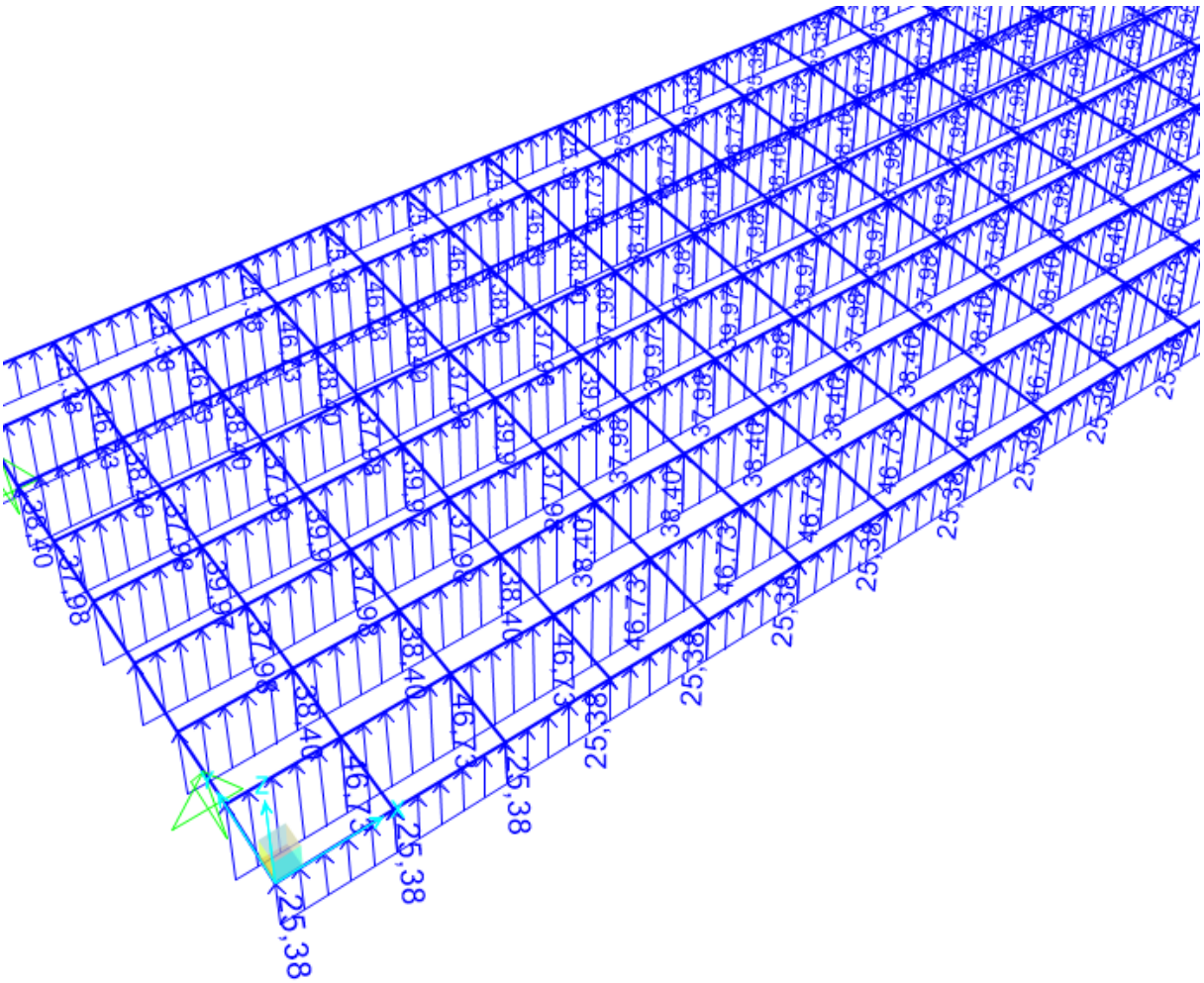

Figure 27: input of prestressed loads induced by tendons on the grillage

Moreover, each tendon is in a self-equilibrium position; as a consequence the vertical component of the prestressed force needs to be input on the model. The vertical component of the force is distributed at the two edges of the span, as shown on figure 27 above. Therefore $2Pv = p * L = 336.947 * 20 = 6\,738.94$ kN

$Pv = 6\,738.94/2 = 3\,369.47$ kN.

This vertical prestressed force is the force at each edge of the grillage. It has to be divided through the tendons and relocated to the members as it has been done previously. Using the same method, table 11 shows the vertical loads which have to be inputted at each edge of members.

Table 11: table showing the vertical loads at each edge of members

Total equivalent load on longitudinal members										
Longitudinal member	1	2	3	4	5	6	7	8	9	Total
Equivalent load (kN)	253,75753	467,26747	384,04932	379,81568	399,69702	379,81568	384,04932	467,26747	253,75753	3369,47700

In order to establish equilibrium conditions, the vertical component of the prestressed force is downward directed as the force exerted by the tendon is uplift directed (figure 30).

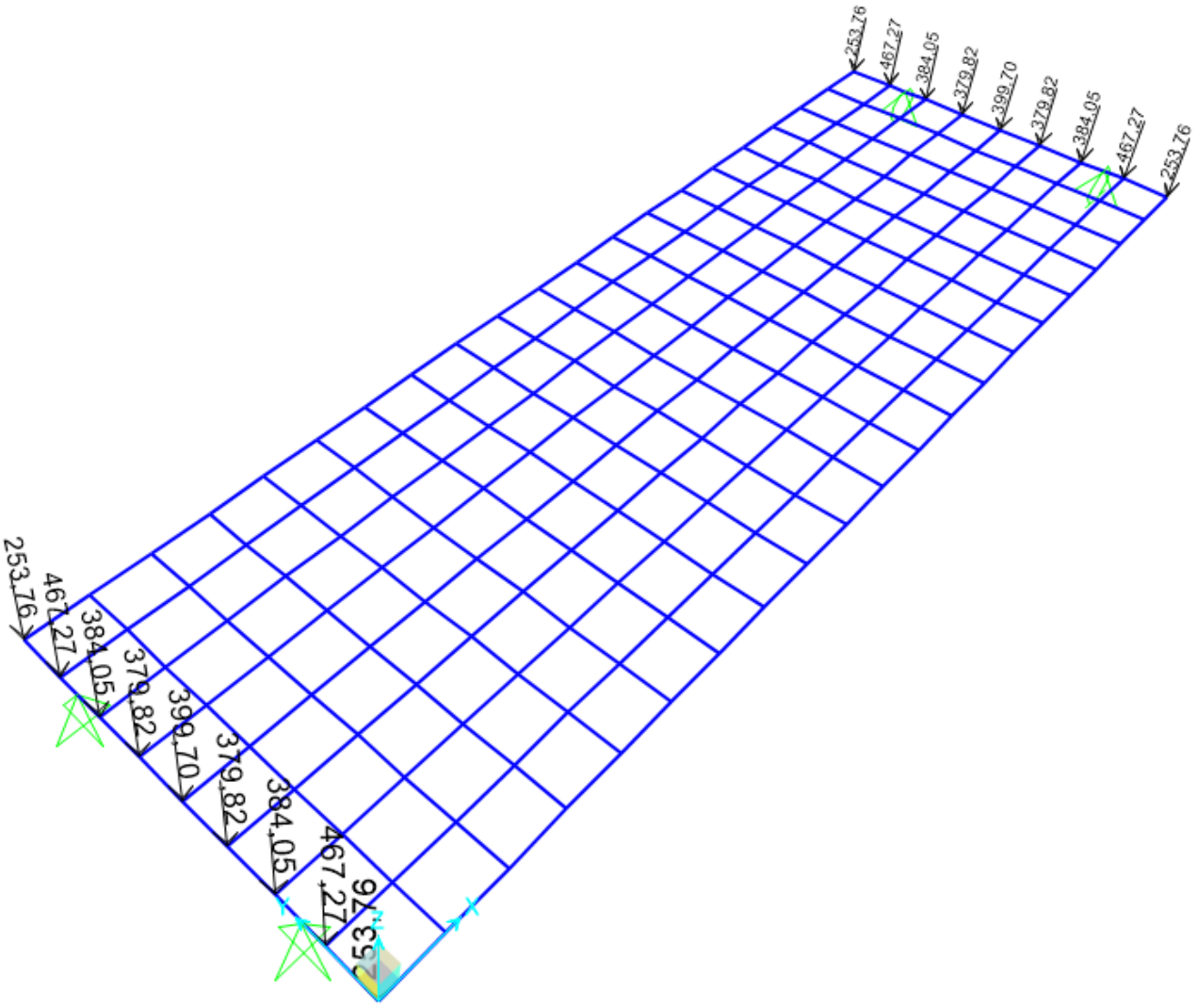

Figure 28: input of the vertical component of the prestressed load on the grillage

4. Verification of the model

Interpreting the results consists first in checking the model. Few simple operations allow the verification of the model, including checking the reactions and the moments.

- Verification of the reactions at support

In order to check if the loads are inputted correctly, the sum of all vertical loads should be equal to the sum of vertical reactions at supports. The sum of vertical loads inputted on the model gathers TS, UDL and prestressed loads.

- TS loads: Σ TS = 1 200 kN

- UDL: Σ UDL = Σ distributed loads * length

= 47 * 20

=940 kN

- Prestressed load:

Distributed loads = -336,947 [kN/m] * 20 [m] = -6 738.94 kN

Punctual loads = 2*3 369,47 = 6 738.94 kN

Due to the self-equilibrium of the prestressed tendons, the sum of prestressed loads should be equal to zero, as verified here.

Therefore, the sum of vertical loads is:

Σ vertical loads = 1 200 + 940 – 6 738.94 + 6 738.94 = <u>2 140 kN</u>

Figure 29 shows the reactions at support after running the analysis of the grillage on SAP 2000.

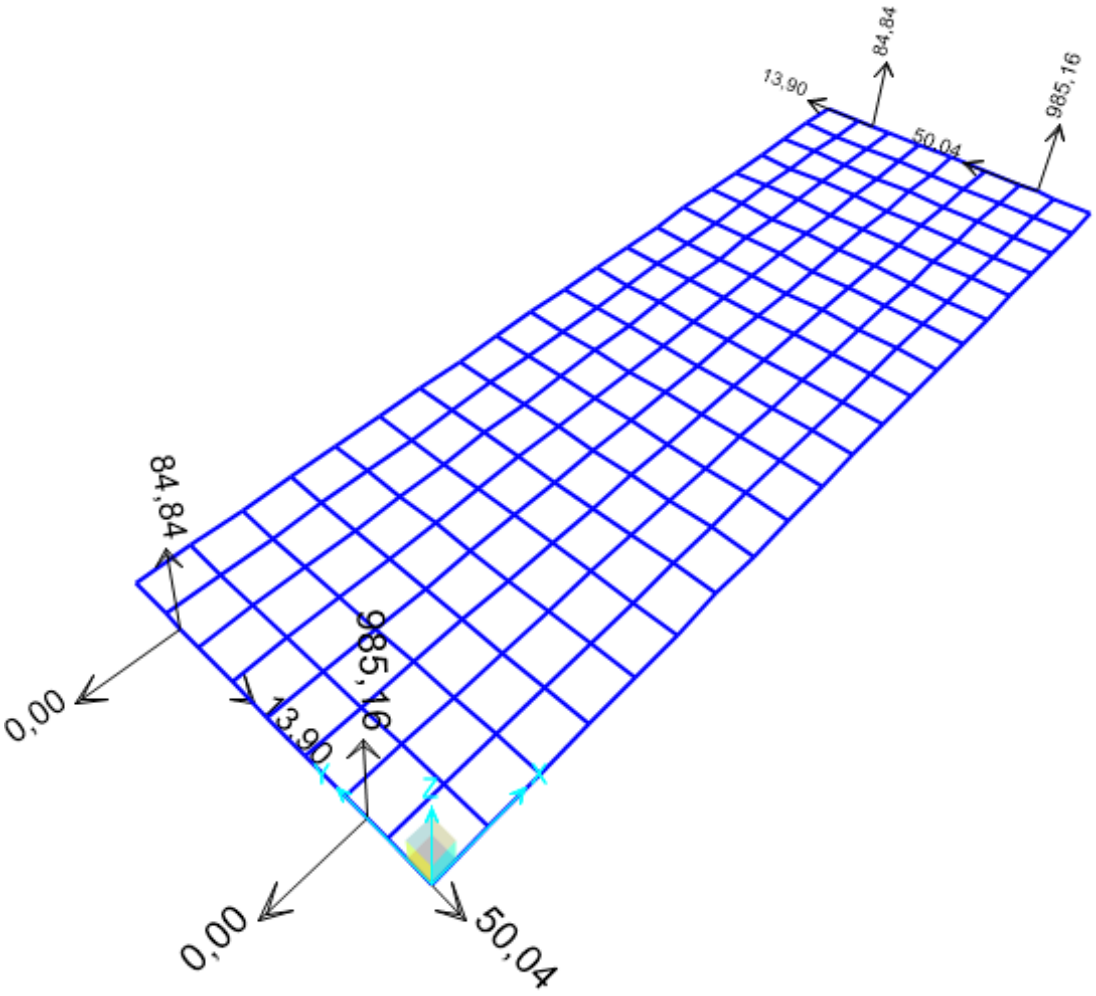

Figure 29: reactions at supports

The sum of the vertical reactions is equal to:

R_v = 84.84 * 2 + 985.16 * 2 = 2 140 kN, therefore, the reactions are correct.

- Verification of moments

  There are two ways to verify if the moments are correct:

The first method consists to check if the sum of the maximum moments at mid span under tandem and UDL loads is equal to the sum of the moments inputted on the grillage. The moments inputted on the grillage are:

- TS loads: M_{TS} = 360*9.4/2 + 480*20/4 + 360*9.4/2 = 5 784 kN.m

- UDL loads: M_{UDL} = 47 * 20^2 / 8 = 2 350 kN.m

=> Total = 8 134 kN.m

Table 12 shows the moments obtained through the grillage analysis at mid span under UDL and tandem loads.

Table 12: table sowing the calculation of the sum of the maximum moments of the grillage

UDL + TS		
Longitudinal member	Maximum moment (kN.m)	Location
1	1668,09	Node 11
2	828,13	Node 11
3	786,03	Node 11
4	757,39	Node 11
5	733,81	Node 11
6	708,77	Node 11
7	683,58	Node 11
8	660,39	Node 11
9	1163,81	Node 11
Total	7990,00	

The difference between the model and the theoretical bending moment is 1.77%. This is due to the errors in readings the obtained moments on the grillage.

The second way to verify the moments includes the prestressed force only. The sum of the bending moments a mid-span under prestressed load only should be equal to the design prestressed force multiplied by the eccentricity:

$$\sum M = P0 * e = 40\,135{,}89 * 0{,}4205 = 16\,877{,}14175\ kN.m$$

Table 13 shows the bending moments obtained at mid-span under prestressed force only.

Table 13: bending moments obtained under prestressed force at mid-span (node 11)

prestressed		
Longitudinal member	Maximum moment (kN.m)	Location
1	-2887,92	Node 11
2	-1579,91	Node 11
3	-1581,82	Node 11
4	-1582,66	Node 11
5	-1582,77	Node 11
6	-1582,66	Node 11
7	-1581,82	Node 11
8	-1579,91	Node 11
9	-2887,92	Node 11
Total	-16847,39	

This represents an error of 0.17% which is due to the accuracy of readings on the grillage. Therefore, the equation is verified and the model is correct.

VI. Stress distribution and robustness analysis

Through the grillage model, it is possible to obtain stresses distribution along the section of the structure. The stress is expressed in function of several parameters, including the moment exerted by loads. Therefore, it is possible to include a load factor in the equation of the stress. This load factor will be computed in function of different load cases which are represented by different level of prestress losses due to corrosion (the loss of prestressed force represents the corrosion on the tendons, reducing the resistance of the bridge). The robustness index of the structure can then be calculated as it is linked to the load factor, which is considered as a performance indicator, thus to the stress of the structure. In this manner, it is possible to include the effect of the corrosion on the structural assessment of the bridge. As exposed in the methodology, three different scenarios will be studied (Figure 30):

a. A loss of prestressed area induced by the corrosion on the three outermost tendons on the left hand side of the structure; up to the complete corrosion of these three tendons;
b. A loss of prestressed area induced by the corrosion on the three tendons located at the centre of the structure; up to the complete corrosion of these three tendons and
c. A loss of prestressed on all the tendons of the structure. The maximum corrosion in this case will be the same in all then tendons and equivalent to the total loss of area of three tendons

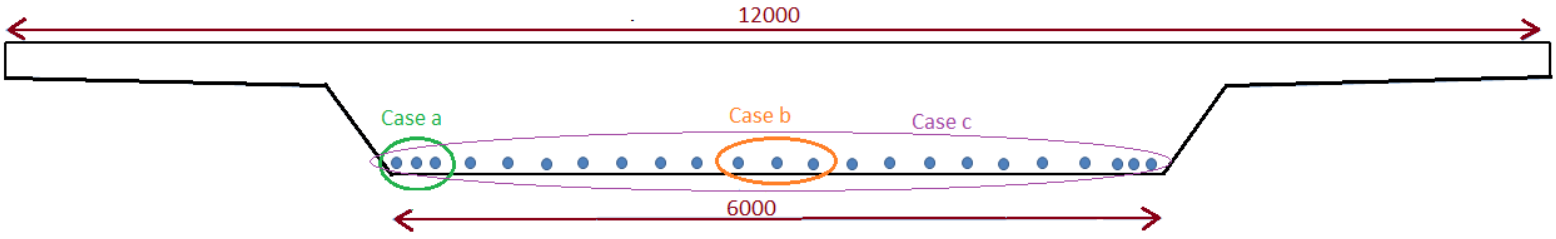

Figure 30: Sketch showing the different study cases

1. Stress distribution calculation

Thanks to the grillage analysis, it is easily possible to compute the stress distribution along the structure. Knowing that the maximum moment occurs at mid span, the stress at the top and at the bottom of the section can be calculated. The stress is a function of the

moment exerted by different loads on the structure, of the distance between the centre of gravity and the bottom or top of section (v' and v respectively), the inertia and the compression stress due to the prestressing force. Hence, the stresses at the top σ1 and at the bottom σ2 are expressed as:

$$\sigma_1 = \frac{M_D * v}{I_{bridge}} + \frac{M_L * v}{I_{member}} - \frac{M_{prestressed} * v}{I_{member}} - \frac{P}{A}$$

$$\sigma_2 = \frac{M_D * v'}{I_{bridge}} + \frac{M_L * v'}{I_{member}} - \frac{M_{prestressed} * v'}{I_{member}} - \frac{P}{A}$$

where M_D is the moment exerted by dead loads;

M_L is the moment exerted by live loads (UDL+TS);

$M_{prestress}$ is the moment in the corresponding member of the grillage exerted by prestressed loads;

v is the distance between the centre of gravity and the top of the section;

v' is the distance between the centre of gravity and the bottom of the section;

I_{bridge} is the inertia of the cross section of the bridge;

I_{member} is the inertia of the corresponding member in the grillage;

P is the total prestressing force and

A is the cross sectional area of the bridge.

The stress distribution can be established, through the results obtained by SAP2000. Indeed, on each longitudinal member the maximum moment (at mid span) can be found which can then give the stress along the equivalent structure. For example, the calculation of the stress at the bottom of the section exerted on the first member is as follow:

$$\sigma_2 = \frac{M_D * v'}{I_{bridge}} + \frac{M_L * v'}{I_{l,ext}} - \frac{M_{prestressed} * v'}{I_{l,ext}} - \frac{P}{A}$$

where M_D is the moment exerted by dead loads:

$M_D = 227{,}442 * 20^2/8 = 11\,372.25$ kN.m

M_L is the moment exerted by live loads (UDL+TS) on the first longitudinal member:

$M_L = 1\,668.09$ kN.m (through grillage analysis on SAP2000)

$M_{prestress}$ is the moment exerted by prestressed loads on the first longitudinal member without any loss: $M_{prestress}$ = 2 887.92 kN.m

v' is the distance between the centre of gravity and the bottom of the section:

v' = 0.575 m

I_{bridge} is the inertia of the cross section of the bridge:

I_{beam} = 0.697499 m^4

$I_{l,ext}$ is the inertia of the first longitudinal member:

$I_{l,ext}$ = 0.1196395 m^4

P is the total prestressing force:

P = 40 135.89 kN and

A is the cross sectional area of the bridge:

A = 8.175 m^2

Therefore:

$$\sigma_2 = \frac{11\,372.25*0.575}{0.697499} + \frac{1\,668.09*0.575}{0.1196395} - \frac{2\,887.92*0.575}{0.1196395} - \frac{40\,135.89}{8.175}$$

σ_2 = -1 397.2 kN/m^2 = -1.3972 Mpa

Table 16 shows the calculations of stresses along the section of the bridge, at top and bottom.

Table 14: calculations of stresses distribution

Longitudinal member	1	2	3	4	5	6	7	8	9
I_{member} (m^4)	0,11964	0,06546	0,06546	0,06546	0,06546	0,06546	0,06546	0,06546	0,11964
$\sigma_{1\,G}$ (Mpa)	6,929338	6,929338	6,929338	6,929338	6,929338	6,929338	6,929338	6,929338	6,929338
M_D (kN.m)	1668,09	828,13	786,03	757,39	733,81	708,77	683,58	660,39	1163,81
$\sigma_{1\,D}$ (Mpa)	5,92562	5,376646	5,103311	4,917366	4,764272	4,6017	4,438153	4,287592	4,134247
M_P (kN.m)	2887,82	1579,91	1581,82	1582,66	1582,77	1582,66	1581,82	1579,91	2887,92
$\sigma_{1\,P}$ (Mpa)	10,25851	10,25759	10,26999	10,27544	10,27616	10,27544	10,26999	10,25759	10,25887
$\sigma_{2\,G}$ (Mpa)	9,374987	9,374987	9,374987	9,374987	9,374987	9,374987	9,374987	9,374987	9,374987
$\sigma_{2\,D}$ (Mpa)	8,017016	7,274286	6,90448	6,652906	6,44578	6,225829	6,00456	5,800859	5,593393
$\sigma_{2\,P}$ (Mpa)	13,87917	13,87791	13,89469	13,90207	13,90304	13,90207	13,89469	13,87791	13,87965
σ_1 (Mpa)	**-2,31314**	**-2,86119**	**-3,14693**	**-3,33833**	**-3,49214**	**-3,65399**	**-3,81209**	**-3,95025**	**-4,10487**
σ_2 (Mpa)	**-1,39675**	**-2,13823**	**-2,52481**	**-2,78377**	**-2,99186**	**-3,21084**	**-3,42473**	**-3,61166**	**-3,82086**

Figure 31 shows the stress distributions along the section of the bridge.

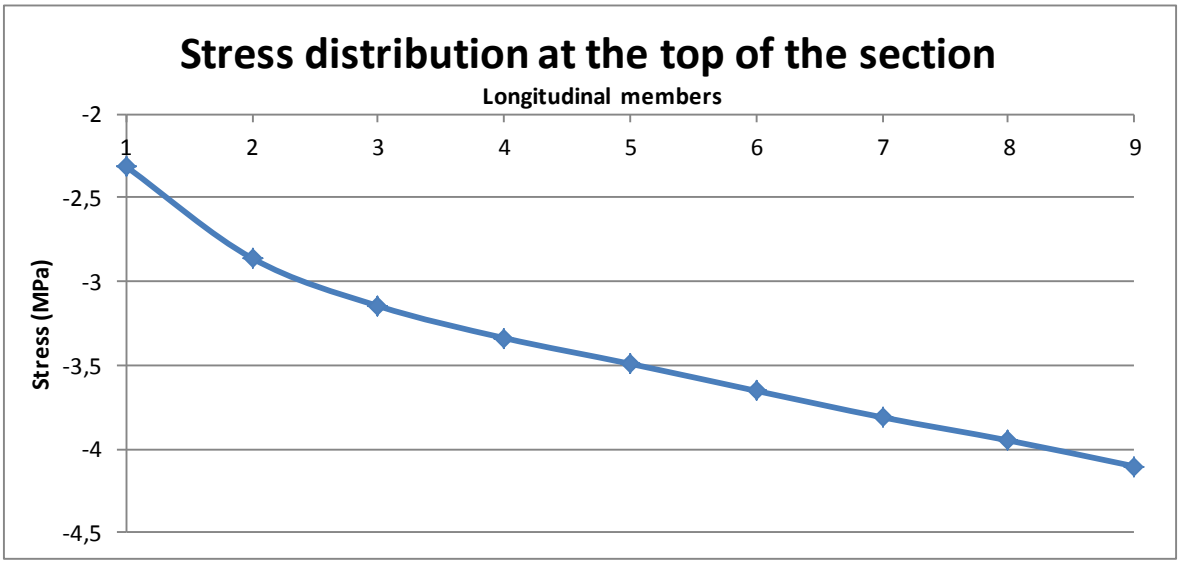

(a)

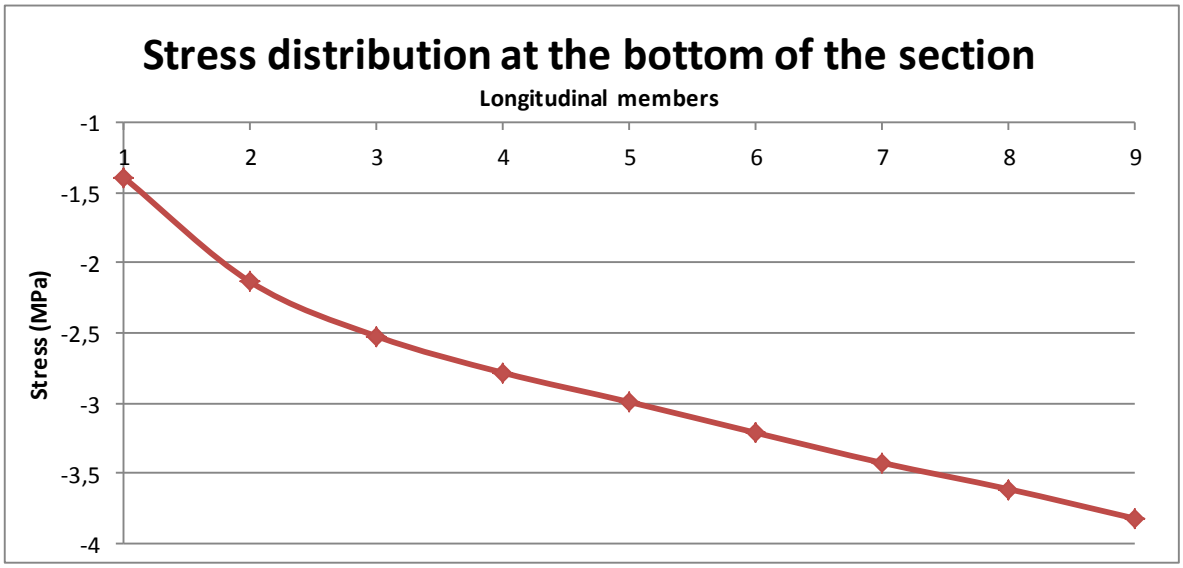

(b)

Figure 31: stress distributions at the top (a) and the bottom (b) of the section

It can be observed that the maximum stress occurs on the first longitudinal member. This is due to the fact that most of live loads are applied on the left hand side of the structure. Indeed, the left and side of the structure is the location of the national lane 1 on which the highest tandem and UDL loads are applied _respectively 600 kN and 9 kN/m². At the top of the section the stress is -2.31314 Mpa and at the bottom -1.39675 Mpa, as shown on figure 32:

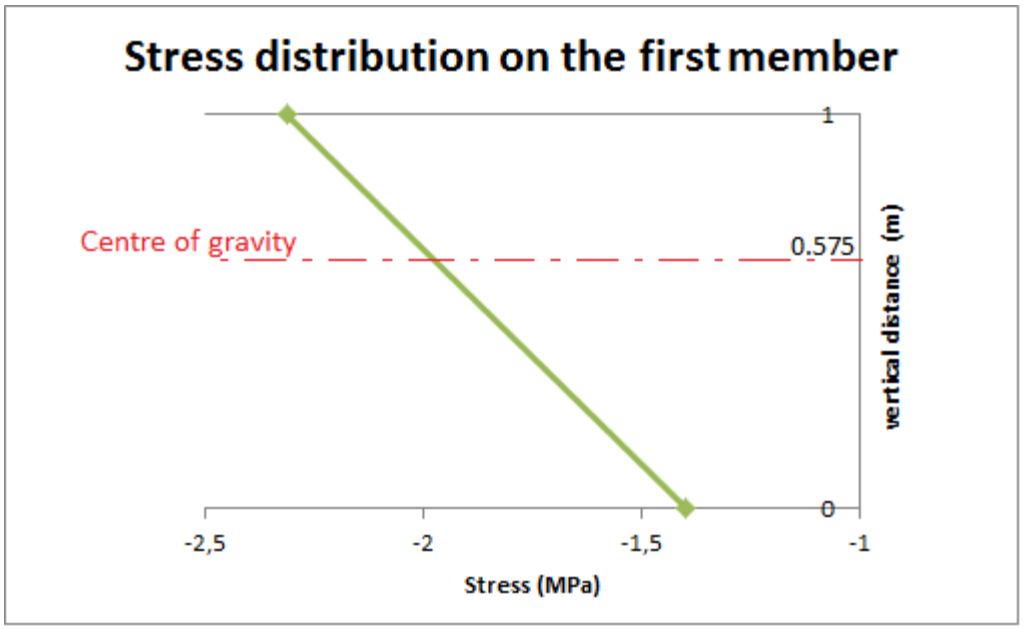

Figure 32: maximum stress distribution (at the first longitudinal member)

The maximum stress is also observed at the bottom of the section (-1.39675 Mpa).

As can be seen, the cross section is under compression in all points, indicating a good design of the prestressing force taking into account the 2-D behaviour of the bridge deck.

As exposed previously, the robustness can be linked to the stress. In order to obtain the maximum robustness index in the structure, it is preferable to express it in function of the maximum stress occurring in the section. Therefore, the robustness will be expressed in function of the stress exerted at the bottom of the section on the first longitudinal member.

2. Load factor

Eduardo Soares Ribeiro Gomes Cavaco defined the robustness index $I_{R,D}$ as an expression of the area below the curve that defines the normalised structural performance f(D) as a function of the normalised damage D:

$$I_{R,D} = \int f(D)dD$$

The normalised damage is the curve representing the load factor in function of different losses of prestress. The load factor γ is a factor of the stress exerted by the live loads when the equation of the maximum stress is equal to zero. In other words, the load factor is expressed in the stress equation and varies in function of the prestress loss. The load factor is the number of times the live load should be increased in order to obtain a stress equal to zero in the most tensioned part of the cross section. The area obtained below

the load factors represents the robustness index which will characterise the structure at different level of losses of prestressed force due to corrosion.

a. Load factor without any loss of prestress

Any loss of prestress means calculations of load factors under all loads on all the members without loss of area of the tendons because of the corrosion. The load factor γ is a factor of the stress exerted by the live loads when the equation of the total stress at the bottom of the section is equal to zero:

$\sigma_{2\ 1st\ member} = 0$

$$\Leftrightarrow \frac{M_D * v\prime}{I_{bridge}} + \gamma \frac{M_L * v\prime}{I_{l,ext}} - \frac{M_{prestressed} * v'}{I_{l,ext}} - \frac{P}{A} = 0$$

$$\Leftrightarrow \boldsymbol{\gamma} = \frac{\frac{P}{A} + \frac{M_{prestressed} * v'}{I_{l,ext}} - \frac{M_D}{I_{bridge}}}{\frac{M_L * v'}{I_{l,ext}}}$$

$$\Leftrightarrow \boldsymbol{\gamma} = \frac{4.909589 + 13.879647 - 9.374987}{8.017016}$$

$\Leftrightarrow \boldsymbol{\gamma} = 1.174283$

Under all loads, without any loss of prestressing force (no effects of the corrosion in the tendons), the load factor is equal to 1.174283. As the load factor is a normalised value ranging from 0 (no resistance) to 1 (maximum resistance), this value has to be the reference value of the load factor. Therefore it is set to 1. All the other load factors will be expressed and scaled in function of this referential value.

b. Loss of prestress on the first three tendons

The first study case (case A) consists of determining the load factor and then the robustness index of the structure after a loss of prestress on the first three members. This has been studied with a loss of 10%, then 20%, 50% and finally 100% of prestressed force exerted by the tendons.

First, the prestressed loads exerted by tendons have been re-calculating in order to obtain the prestressed loads applied on members after a percentage of loss (table 15).

Table 15: prestressed loads calculations on members after loss of prestressed force exerted by the first three tendons (case A)

10 % of loss of prestressed on tendons 1 to 3				20 % of loss of prestressed on tendons 1 to 3			
Prestressed tendon	Load (kN)	Grillage member	Equivalent load on grillage member (kN)	Prestressed tendon	Load (kN)	Grillage member	Equivalent load on grillage member (kN)
1	13,18491	1	22,88033	1	11,71992	1	20,38490
2	13,18491	2	44,82720	2	11,71992	2	42,92766
3	13,18491	3	38,40493	3	11,71992	3	38,40493
4 to 24	14,6499	4	37,98157	4 to 24	14,6499	4	37,98157
		5	39,96970			5	39,96970
		6	37,98157			6	37,98157
		7	38,40493			7	38,40493
		8	46,72675			8	46,72675
		9	25,37575			9	25,37575

50 % of loss of prestressed on tendons 1 to 3				100 % of loss of prestressed on tendons 1 to 3			
Prestressed tendon	Load (kN)	Grillage member	Equivalent load on grillage member (kN)	Prestressed tendon	Load (kN)	Grillage member	Equivalent load on grillage member (kN)
1	7,32495	1	12,89863	1	0	1	0,42150
2	7,32495	2	37,22902	2	0	2	27,73130
3	7,32495	3	38,40493	3	0	3	38,40493
4 to 24	14,6499	4	37,98157	4 to 24	14,6499	4	37,98157
		5	39,96970			5	39,96970
		6	37,98157			6	37,98157
		7	38,40493			7	38,40493
		8	46,72675			8	46,72675
		9	25,37575			9	25,37575

After replacing those prestressed loads on the grillage model on SAP2000, new moments due to prestressing could be obtained. Moreover, it is also important to no forget that the compression stress has also changed as the prestressed load has decreased. The calculation of the compression stress in function of the loss is:

$$\sigma_c = \frac{Ploss}{A}$$

$$= \frac{20\ tendons + \%\ of\ loss\ on\ 3\ tendons}{all\ tendons} * \frac{P}{A}$$

For example, for a loss of prestress of 10 % on 3 tendons:

$$\sigma_c = \frac{20+3*0,9}{23} * \frac{40\ 135.89}{8.175}$$

= 4 845,551 kN/m² = 4.84551 MPa

Table 16 display the compression stresses P/A in function of the percentage of loss for cases A and B _similar percentage of loss of prestress.

Table 16: compression stresses in function of the associated loss of prestressed force

	% of loss on 3 tendons	P/A (Mpa)
Cases A and B	0	4,909589
	10	4,845551
	20	4,781513
	50	4,589398
	100	4,269208

All the parameters are now adjusted which allows the calculation of the corresponding stresses of the structure and the load factors (table 17).

Table 17: load factors calculations under a loss of prestressed on the first three tendons

Case A: loss on tendons 1 to 3				
% of loss	Mp (kN/m)	$\sigma_{2\,p}$ (Mpa)	Y_{real}	**$\gamma_{adjusted}$**
0	2887,92	13,879647	1,174283	**1**
10	2844,32	13,670101	1,140158	**0,970939**
20	2800,91	13,461468	1,106146	**0,941976**
50	2670,39	12,834175	1,003938	**0,854937**
100	2452,87	11,788751	0,833598	**0,709878**

c. Loss of prestress on the three tendons at mid-span

The second study case consists of a loss of prestressed on the middle tendons _tendons 10, 11 and 12. The same methodology is applied: after a loss of 10%, 20%, 50% and 100% of prestressing force of tendons the moments are calculating again on SAP2000 allowing the calculation of the load factors.

Table 18 shows the calculations of prestressed loads after a loss of prestress force on tendons 10 to 12.

Table 18: prestressed loads calculations for case study B

10 % of loss of prestressed on tendons 10 to 12				20 % of loss of prestressed on tendons 10 to 12			
Prestressed tendon	Load (kN)	Grillage member	Equivalent load on grillage member (kN)	Prestressed tendon	Load (kN)	Grillage member	Equivalent load on grillage member (kN)
10	13,18491	1	25,37575	10	11,71992	1	25,37575
11	13,18491	2	46,72675	11	11,71992	2	46,72675
12	13,18491	3	38,40493	12	11,71992	3	38,40493
1-9;13-23	14,6499	4	36,31758	1-9;13-23	14,6499	4	34,65359
		5	37,23872			5	34,50774
		6	37,98157			6	37,98157
		7	38,40493			7	38,40493
		8	46,72675			8	46,72675
		9	25,37575			9	25,37575

50 % of loss of prestressed on tendons 10 to 12				100 % of loss of prestressed on tendons 10 to 12			
Prestressed tendon	Load (kN)	Grillage member	Equivalent load on grillage member (kN)	Prestressed tendon	Load (kN)	Grillage member	Equivalent load on grillage member (kN)
10	7,32495	1	25,37575	10	0	1	25,37575
11	7,32495	2	46,72675	11	0	2	46,72675
12	7,32495	3	38,40493	12	0	3	38,40493
1-9;13-23	14,6499	4	29,66162	1-9;13-23	14,6499	4	21,34167
		5	26,31480			5	12,65990
		6	37,98157			6	37,98157
		7	38,40493			7	38,40493
		8	46,72675			8	46,72675
		9	25,37575			9	25,37575

Table 19 shows the calculation of load factors of case study B.

Table 19: load factors calculation of case study B

Case B: loss on tendons 10 to 12				
% of loss	Mp (kN/m	$\sigma_{2\,p}$ (Mpa)	Y	**$\gamma_{adjusted}$**
0	2887,92	13,87965	1,174283	**1**
10	2844,21	13,66957	1,140092	**0,970883**
20	2806,02	13,48603	1,10921	**0,944584**
50	2691,44	12,93534	1,016557	**0,865683**
100	2500,48	12,01757	0,86214	**0,734184**

d. Loss of prestress on all the tendons

The third case study consists of a loss of prestressed area on all the tendons, uniformly distributed. In order to obtain comparable results with the two other case studies, the maximum loss of prestressed force is taken as the maximum loss of the other case studies. This relates to 100% of loss of three tendons which is equivalent to a loss of 3 tendons over 23, corresponding to:

$$\frac{3}{23} = 13.04\%$$

In order to obtain a gradual load factor curve, a loss of half a tendon will be studied, and then a loss of 1, 2 and finally 3 tendons _which corresponds to the maximum loss of 13.04%. As the two other case studies, the same methodology is followed. Therefore, table 20 shows the calculations of the prestressed loads after loss of prestressed force on all tendons.

Table 20: prestress loads calculation for case study C

2,17 % (=0,5 tendon) of loss of prestressed on all tendons				**4,35 % (=1 tendon) of loss of prestressed on all tendons**			
Prestressed tendon	Load (kN)	Grillage member	Equivalent load on grillage member (kN)	Prestressed tendon	Load (kN)	Grillage member	Equivalent load on grillage member (kN)
All	14,33200	1	24,82510	All	14,01263	1	24,27191
		2	45,71279			2	44,69414
		3	37,57155			3	36,73432
		4	37,15737			4	36,32937
		5	39,10270			5	38,23102
		6	37,15737			6	36,32937
		7	37,57155			7	36,73432
		8	45,71279			8	44,69414
		9	24,82510			9	24,27191

8,70 % (=2 tendons) of loss of prestressed on all tendons				13,04 % (=3 tendons) of loss of prestressed on all tendons			
Prestressed tendon	Load (kN)	Grillage member	Equivalent load on grillage member (kN)	Prestressed tendon	Load (kN)	Grillage member	Equivalent load on grillage member (kN)
All	13,37536	1	23,16806	All	12,73955	1	22,06675
		2	42,66152			2	40,63357
		3	35,06371			3	33,39692
		4	34,67717			4	33,02876
		5	36,49234			5	34,75764
		6	34,67717			6	33,02876
		7	35,06371			7	33,39692
		8	42,66152			8	40,63357
		9	23,16806			9	22,06675

The compression stresses are not the same as cases A and B as the percentage of loss is not gradually similar. Table 21 shows the calculation of the compression stresses in function of the percentage of loss of prestress.

Table 21: compression stresses in function of the associated loss of prestressed force for case C

	% of loss on all tendons	P/A (Mpa)
Case C	0	4,909589
	2,173913043	4,802859
	4,347826087	4,696129
	8,695652174	4,482668
	13,04347826	4,269208

All the parameters are corrected adjusted in order to calculate the load factors. Table 22 shows the calculations of the load factor for case study C.

Table 22: load factor calculations of case study C

Case C: loss on all tendons						
number of lost tendons	**% of loss**	**Equivalent % of loss**	Mp (kN/m)	$\sigma_{2\,p}$ (Mpa)	Y_{real}	**$\gamma_{adjusted}$**
0	**0,00**	**0,00**	2887,92	13,879647	1,174283	**1**
0,5	**2,17**	**16,67**	2825,26	13,578496	1,123407	**0,956674**
1	**4,35**	**33,33**	2762,3	13,275904	1,07235	**0,913195**
2	**8,70**	**66,67**	2636,67	12,672113	0,97041	**0,826385**
3	**13,04**	**100,00**	2511,34	12,069764	0,868651	**0,739728**

3. Results

Now the load factors are obtained for the three different cases, it is possible to plot the results on a graph. Load factors, ranging on a scale from 0 to 1, are plotted versus the percentage of loss of prestressed force on the three concerned tendons. The obtained curve defines the normalised structural performance f(D) as a function of the normalised damage D. Hence, the area obtained below the curve represents the robustness index $I_{R,D}$ (Figures 23, 24 and 25):

$$I_{R,D} = \int f(D)dD$$

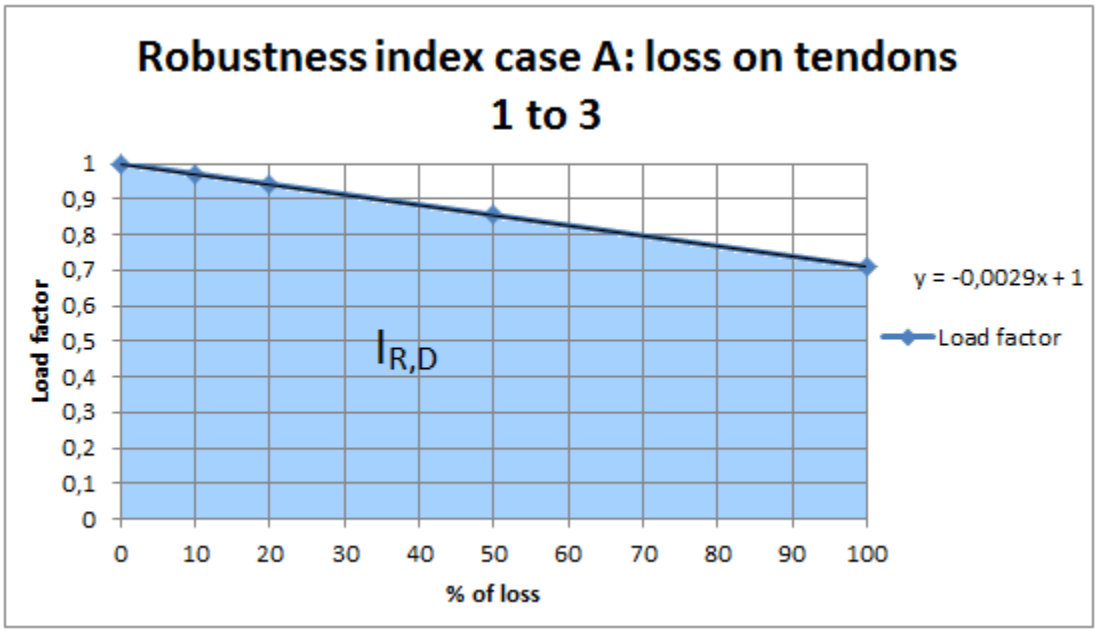

Figure 33: graph showing the robustness index of case study A

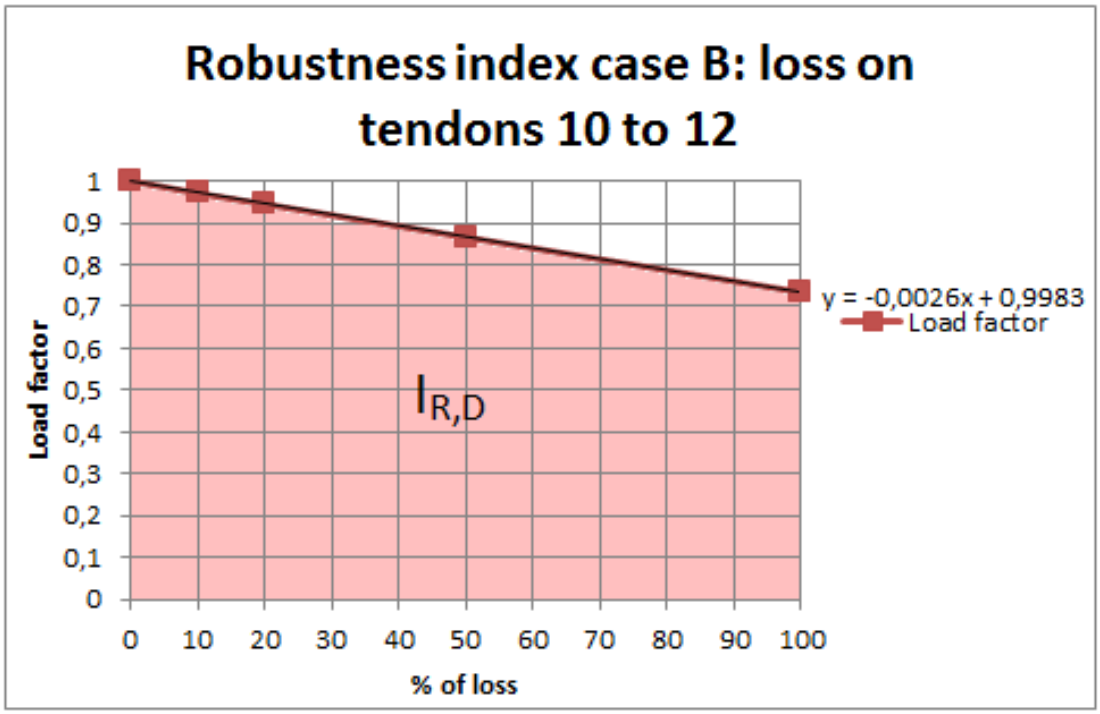

Figure 34: graph showing the robustness index of case study B

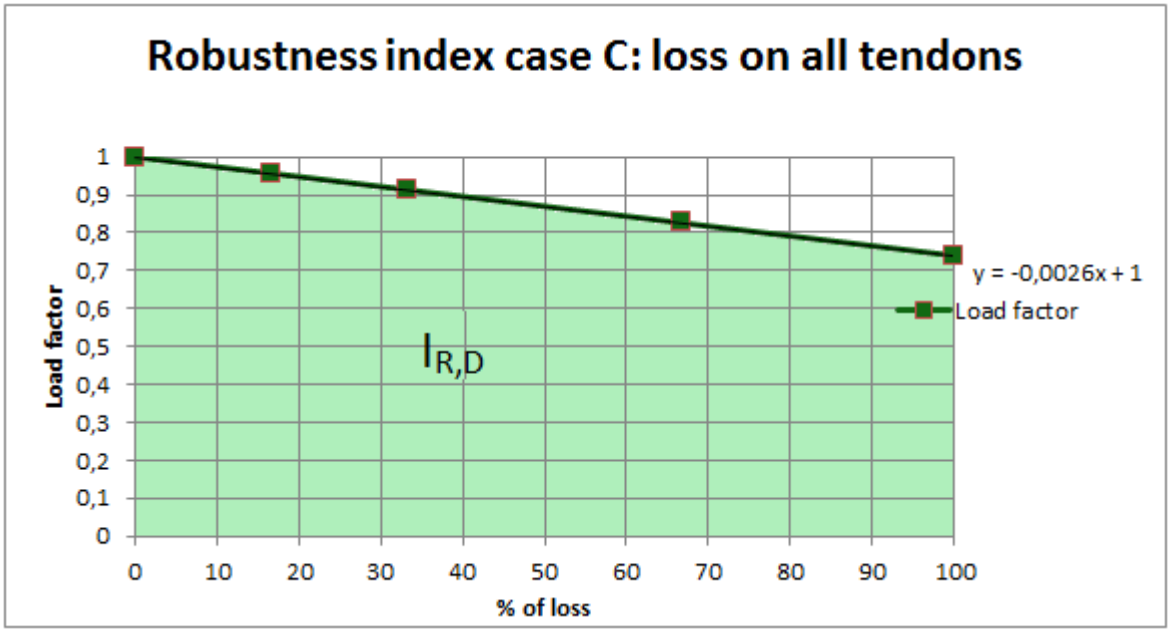

Figure 35: graph showing the robustness index of case study C

In order to obtain the robustness index _representing by the area below the curve_ a trend line was drawn and its equation was obtained. It is now possible to integrate this equation and therefore obtain the index of robustness for each case study.

- Case A: the equation of the trend line is f(D) = -0.0029x+1

  As $I_{R,D(A)} = \int f(D)dD$ thus:

$I_{R,D(A)} = \int(-0.0029 * D + 1)\, dD$

$I_{R,D(A)} = [-0.0029 * D\text{^}2/2 + 1 * D]_{0\%}^{100\%}$

$I_{R,D(A)} = \frac{-0.0029*100^2}{2} + 100$

$I_{R,D(A)} = 85.5\% = 0.855$

The index of robustness of the structure is 0.855 for a loss of prestress on the first three members.

- Case B: the equation of the trend line is f(D) = -0.0026x+0.9983

  As $I_{R,D(B)} = \int f(D)dD$ thus:

  $I_{R,D(B)} = \int(-0.0026 * D + 0.9983)\, dD$

  $I_{R,D(B)} = [-0.0026 * D\text{^}2/2 + 0.9983 * D]_{0\%}^{100\%}$

  $I_{R,D(B)} = \frac{-0.0026*100^2}{2} + 0.9983 * 100$

  $I_{R,D(B)} = 86.83\% = 0.8683$

The index of robustness of the structure is 0.8683 for a loss of prestress on the middle three members.

- Case C: the equation of the trend line is f(D) = -0.0026x+1

  As $I_{R,D(C)} = \int f(D)dD$ thus:

  $I_{R,D(C)} = \int(-0.0026 * D + 1)\, dD$

  $I_{R,D(C)} = [-0.0026 * D\text{^}2/2 + 1 * D]_{0\%}^{100\%}$

  $I_{R,D(C)} = \frac{-0.0026*100^2}{2} + 1 * 100$

  $I_{R,D(C)} = 87\% = 0.87$

The index of robustness of the structure is 0.87 for a loss of prestress on all the members.

Table 23 summarises the results of index of robustness of each case.

Table 23: summary of results of index of robustness

	Case A	Case B	Case C
$I_{R,D}$	0,855	0,8683	0,87

4. Analysis

a. Load factors

It can be seen that load factors values decrease with an increase of loss of prestressed force. This trend was expected as the load factor depends on the moment exerted by all loads on the structure. Consequently, when loads decrease the load factors lower too. This is verified for all cases, as load factors run from 1 to 0.709878 for case A, from 1 to 0.73418 for case B and from 1 to 0.73973 for case C.

However, the load factor is not equal to the remaining percentage of prestressed load as shown on table 24. The remaining percentage of prestressed load is equal to the load of 20 tendons and the remaining percentage of load on the three tendons $\frac{20+x\%*3}{23}$ for cases A and B. For case C it is equal to the number of remaining tendons: $\frac{20+x}{23}$.

Table 24: comparison between the load factor and the percentage of remaining prestressed load

Case A		Case B		Case C	
$\gamma_{adjusted}$	% remaining prestresed area	$\gamma_{adjusted}$	% remaining prestresed area	$\gamma_{adjusted}$	% remaining prestresed area
1	100,00	1,00000	100,00	1,00000	100,00
0,970939	98,70	0,97088	98,70	0,95667	97,83
0,941976	97,39	0,94458	97,39	0,91320	95,65
0,854937	93,48	0,86568	93,48	0,82639	91,30
0,709878	86,96	0,73418	86,96	0,73973	86,96

This difference is explained by the fact that the load factor is not only a function of the prestressed area. It is not directly proportional to it as it also depends on the other loads and the location of the applied loss of prestress. Indeed, the load factors are calculated for a stress on the first longitudinal member (as this is where the stress is the maximum one) even if the losses of prestressed loads are at the middle or on the opposite side of the structure. Moreover, the load factor depends on dead loads, live loads and prestressed loads and the compression factor due to the prestressed force. Dead and live loads do not vary but prestressed loads and prestressed forces depend on the percentage of loss of prestressing and where this loss is produced _location of the tendons within the cross section.

As a conclusion, load factors trends are as expected: decreasing when the loss of prestress is increasing; but not proportional to the percentage of remaining prestressed loads. Also for this reason, the effect of the prestressing in the bridge was also modelled

through the use of the grillage, by the use of the equivalent prestressing force exerted by each tendon, and not assuming a global behaviour as a beam. Only in this way, the hyper static effect in the transversal direction could be taken into account.

b. Index of Robustness

The higher the robustness index, the less sensitive to the damage the structure is. Therefore, the structure is the most robust when the loss of prestress occurs on all the tendons: case C where $I_{R,D}$ = 0,87. The loss of prestress is spread uniformly along the structure; all the tendons are thus affected at the same level by corrosion. The area of prestressed is reduced independently with the live loads; as a consequence the highest area of prestress is still spread at the edges where most of the live loads are applied. This case is thus the best case as the index of robustness is affected on all the structure, and not at a high loaded area.

The structure is the less robust when the loss of prestress is spread on the first three tendons: case A where $I_{R,D}$ = 0,855. This might be explained by the fact that most of the loadings _live loads particularly_ are applied on the left edge of the section and are not equally distributed along the section. Therefore, the bridge is less tolerant to the damage occurring close to this zone.

The robustness index in case B is also high comparing to case A. Case B corresponds to a loss of prestress on the middle tendons. The robustness of the structure is not considerably affected for this case as most of the loadings are located near the edge and not on the middle tendons. The robustness index for case B is close to the one of case C _respectively 0,8683 and 0,87. This proves again that the robustness index depends on where the loads are distributed and which corresponding tendons are affected by the loss of prestress. Figure 36 compares the robustness index of all cases. It can be seen that the smallest one is case A delimited by the blue curve, following by case B in red and finally by case C in green which has the highest robustness index.

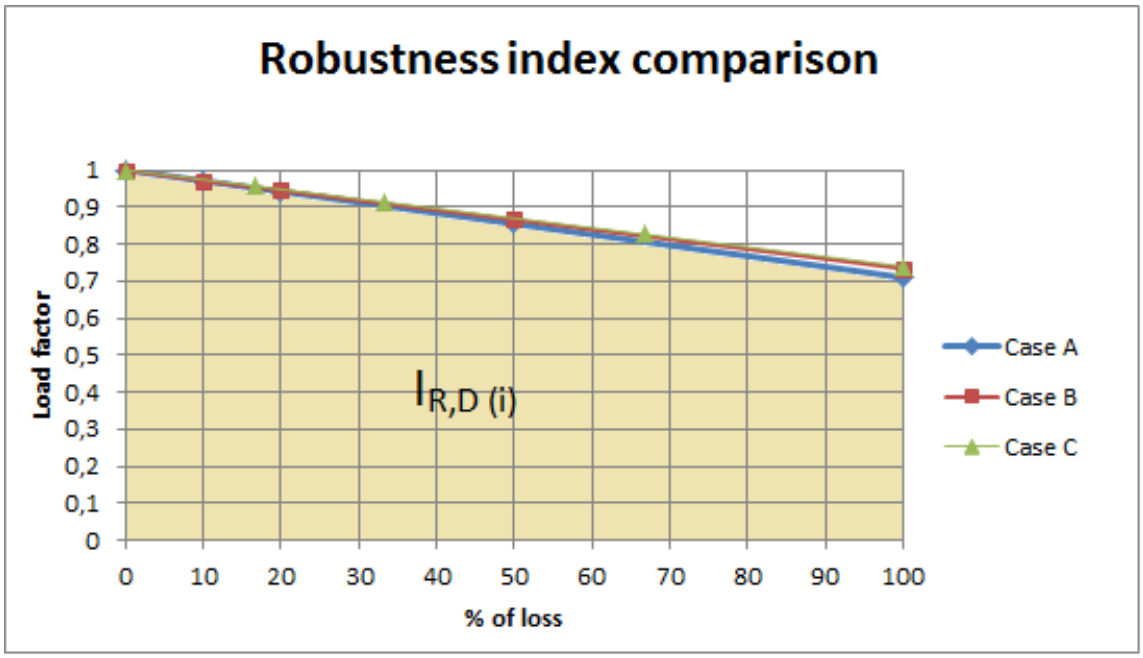

Figure 36: graph comparing the robustness indexes

To summarise, the highest robustness index appears when the loss of prestress induced by corrosion occurs uniformly on all the tendons. Therefore, the prestressed force is still spread along the structure in function of the loadings. This is also verified by the case where corrosion affects the first three tendons, which is also the location of the highest loadings. In this case, the index of robustness is the lowest. Robustness is highly linked to a loss of prestress force on tendons which receive the highest loadings.

However, as the robustness indexes are very similar in all cases _maximum 1,5% of difference_ it can conclude that the massive slab bridge type is very robust to damage appearing in any of the prestressing tendons or, in other words, this type of bridge is low sensitive to where the corrosion in the tendons occur.

CONCLUSION

The objectives of this thesis were first to get familiar with post tensioned bridges, robustness and corrosion effect on post tensioned bridges. Following Eurocode and through the literature review, those concepts have been exposed. The use of the grillage analysis aided by the software SAP2000 helped in analysing the behaviour of the bridge in function of different exposure and scenario cases. Three case studies have been considered, linking the effect of corrosion on the robustness of the structure at three different locations. Case A was considering a loss of prestress area due to corrosion on the first three tendons _which were the most loaded tendons. Case B referred to corrosion on the three middle tendons while case C was considering a loss of prestress area on all the tendons.

The robustness indexes have been calculated for each case following Eduardo Soares Ribeiro Gomes Cavaco's methodology. As a result, the robustness of the post tensioned bridge has been qualified and quantified. It has been demonstrated that the corrosion affect the most the robustness of the post tensioned bridge when it appears on the most loaded tendons, which correspond to case A. Moreover, the corrosion affect the less the robustness aspect of the structure when it is spread uniformly on all the tendons.

As the robustness indexes were found really closed to each other for the three cases, it has been demonstrated that post tensioned bridge does not react that much to corrosion. Indeed, the difference in robustness between cases was less than 1.5% which proves that whenever the corrosion occurs, this type of bridge stays robust enough to withstand corrosion problems.

APPENDIXES

Appendix I: Cross section of the bridge

Appendix II: Autocad drawing showing the variable loads

Appendix III: Prestressed tendons distribution

Appendix IV: Cross section of the bridge with its equivalent grillage model view

Appendix V: Plan view of the equivalent grillage

Appendix VI: Equivalent grillage and the location of loads

Appendix VII: the distribution of UDL loads on the grillage

Appendix VIII: Tendon's shape along the bridge

Appendix I: Cross section of the bridge

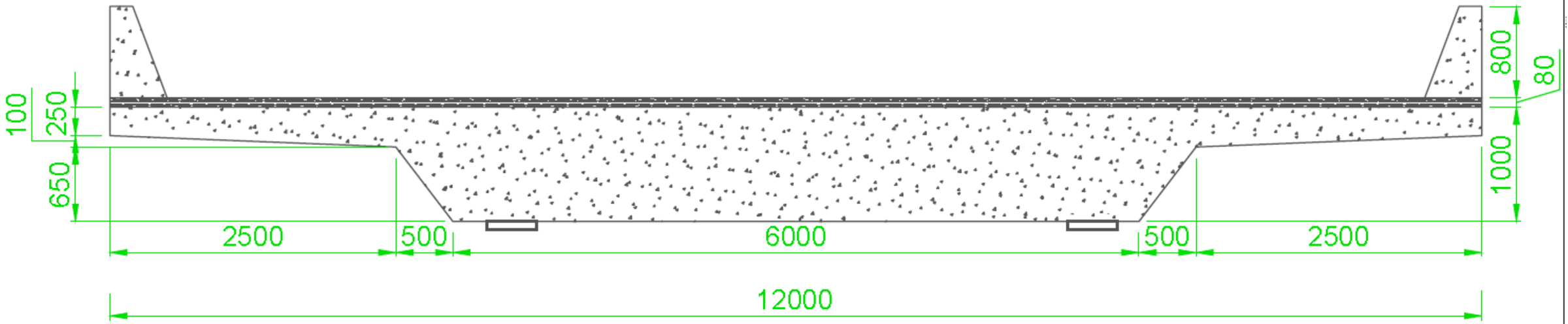

Cross section of the bridge

Scale:1:50

Christelle GRANGE

Civil engineering department

Appendix II: Autocad drawing showing the variable loads

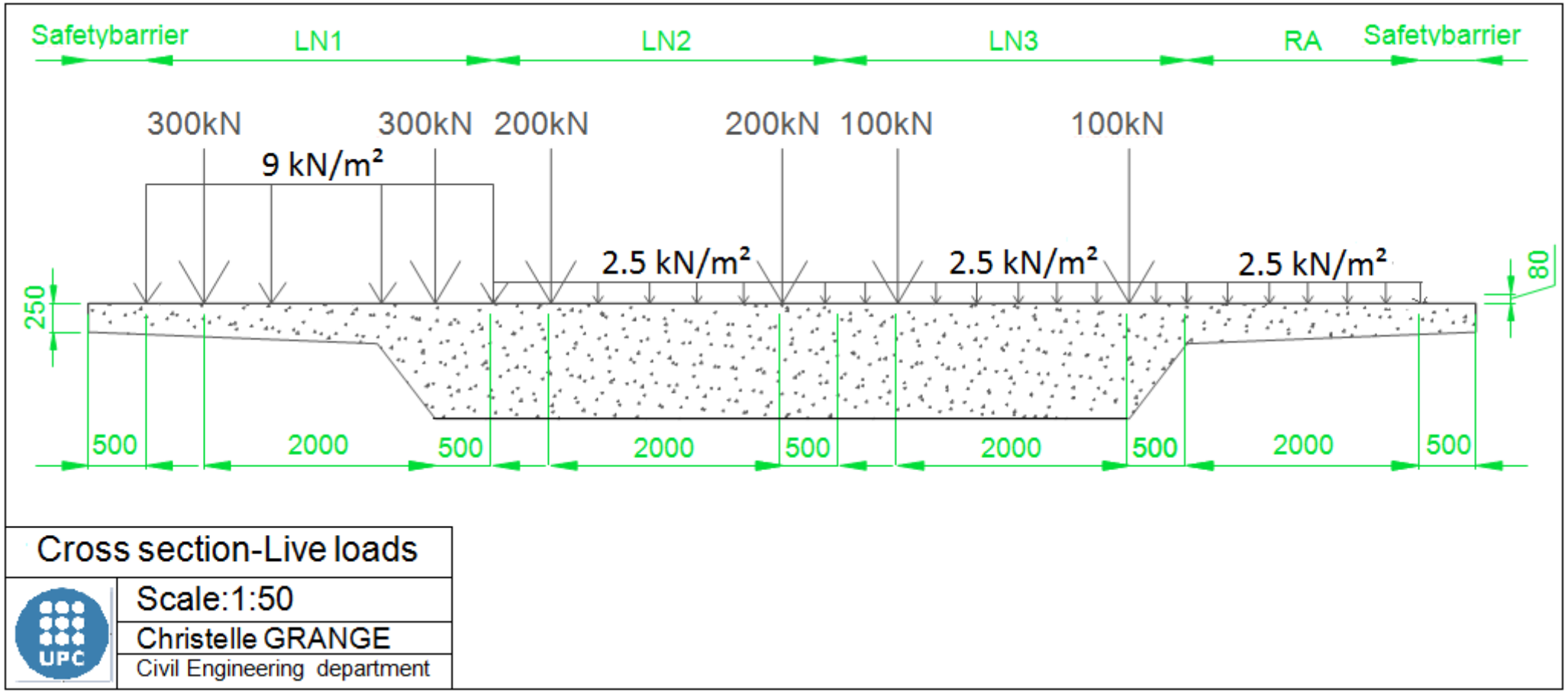

Appendix III: Prestressed tendons distribution

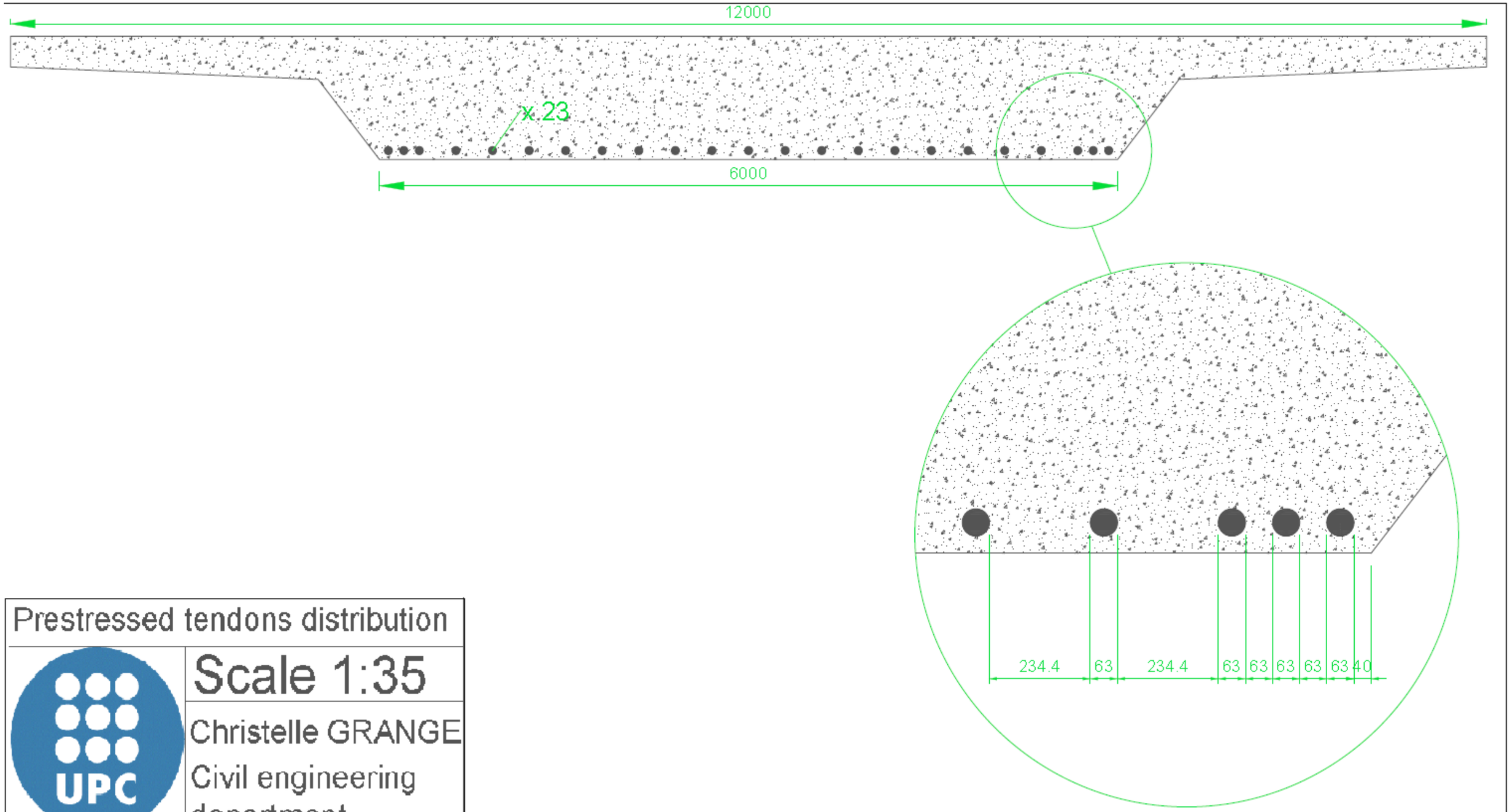

Prestressed tendons distribution

Scale 1:35

Christelle GRANGE
Civil engineering department

Appendix IV: Cross section of the bridge with its equivalent grillage model view

Appendix V: Plan view of the equivalent grillage

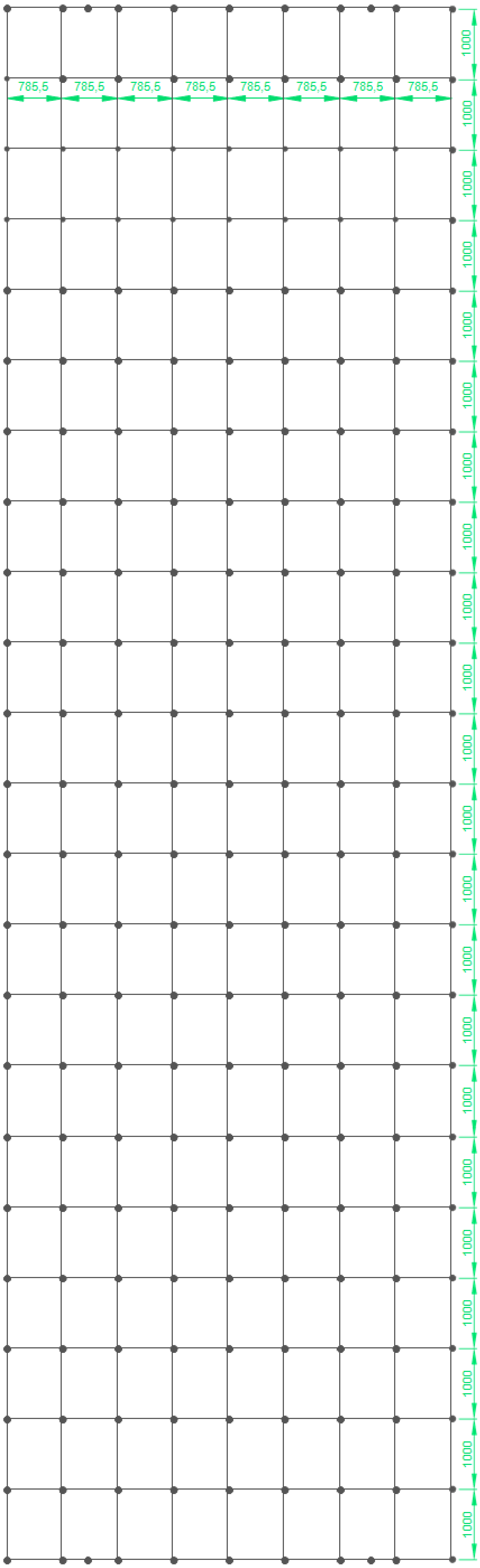

Equivalent grillage-Plan view

UPC

Scale1:60

Christelle GRANGE

Civil engineering department

Appendix VI: Equivalent grillage and the location of loads

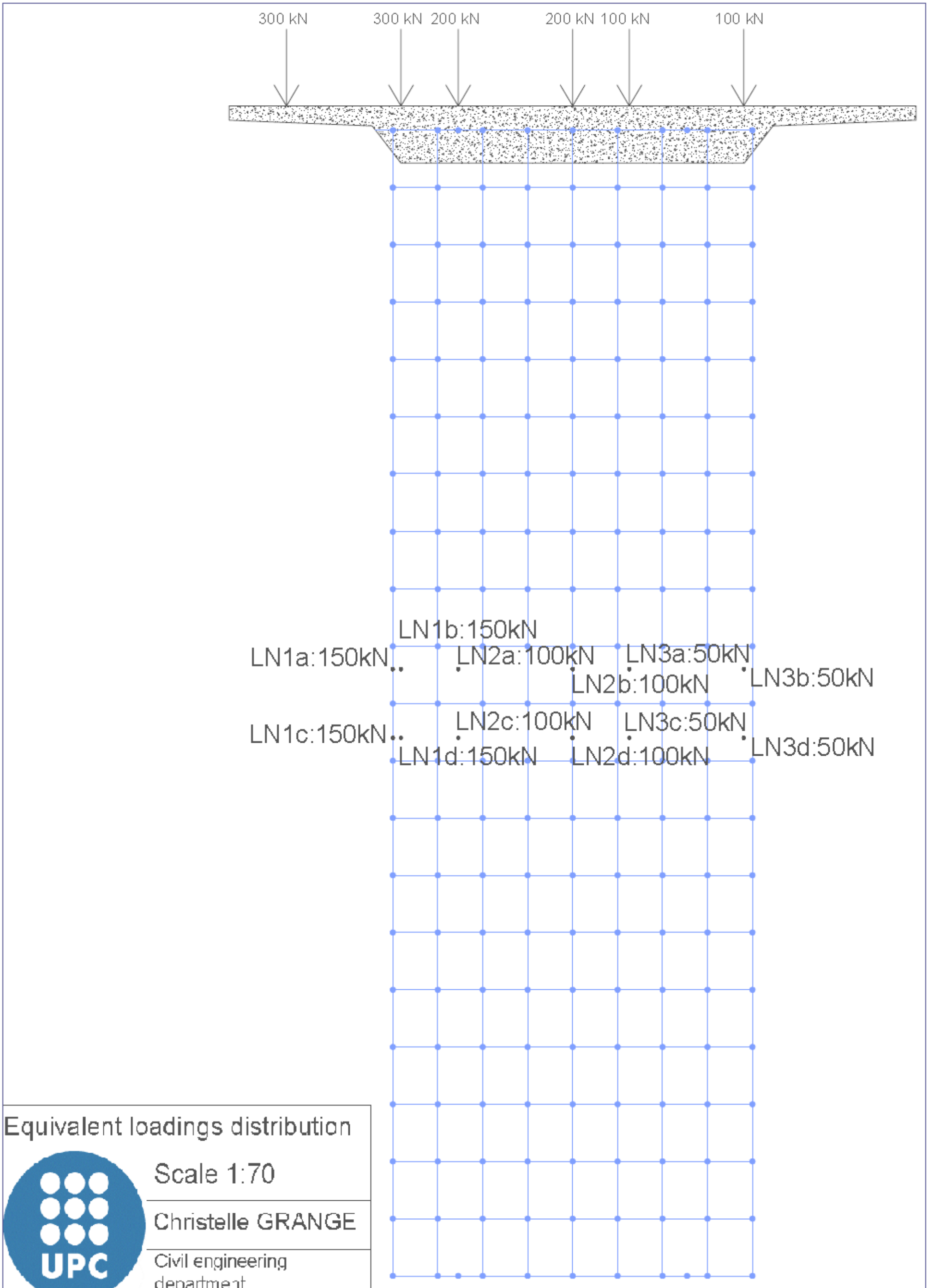

Equivalent loadings distribution

Scale 1:70

Christelle GRANGE

Civil engineering department

Appendix VII: the distribution of UDL loads on the grillage

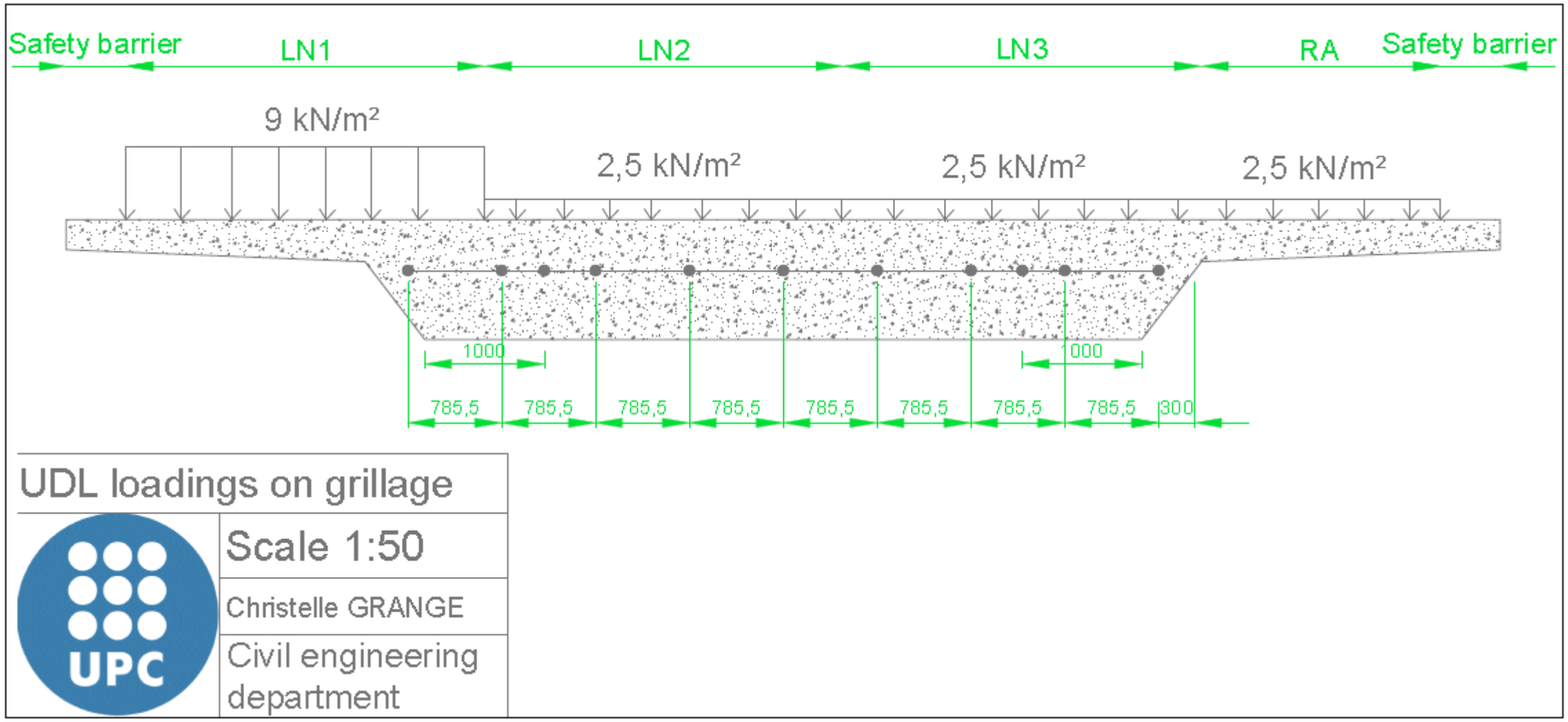

Appendix VIII: Tendon's shape along the bridge

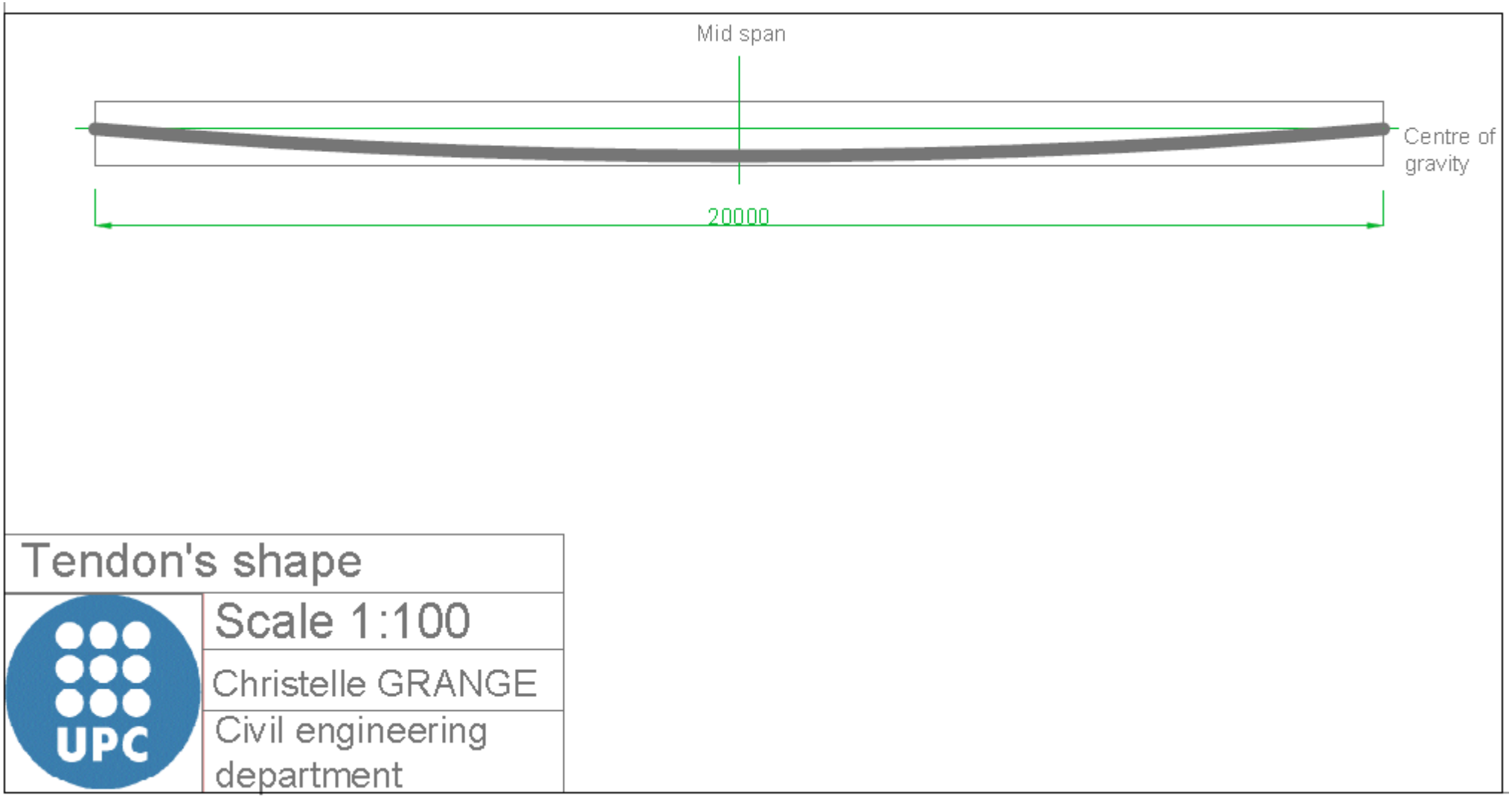

REFERENCES

- Amlan Sengupta and Prof. Menon (2011). Prestressed concrete structures. Indian Institute of Technology Madras

- Andrew A E, Turner F H (1991). Post-tensioning systems for concrete in the UK: 1940-1985. London: Ciria report.

- American STM A-416 Standard, strand for prestressed concrete.

- Baker J.W., Schubert M., Faber M.H. On the assessment of robustness. Structural Safety, Vol. 30, No. 3, 2008, pp. 253-267

- Bijan (2000). Layout of post tensioning and passive reinforcement in floor slabs. Phoenix, Arizona: Aalami.

- Biondini, Restelli and Frangopol (2008) On structural robustness, redundancy and static indeterminacy, American society of civil engineers, pp1-10.

- BS EN 1992-1-1:2004 Design of concrete structures. General rules and rules for buildings.

- EN 1991-2: 2003 Loads on bridges

- Corven John, Moreton Alan (2013-5). Post-Tensioning Tendon Installation and Grouting Manual. 2nd ed. Washington: Federal Highway Administration.

- Dennis Mertz (2012). Steel bridge design handbook - Redundancy. Washington D.C.: Federal Highway Administration.

- Eduardo Cavaco, Joan R. Casas and Luis Neves (2011). Quantifying redundancy and robustness of structures. Proceedings of IABSE Workshop on Safety, Failures and Robustness of Large Structures. Helsinki (Finland)

- Eduardo Soares Ribeiro Gomes Cavaco (2013). Robustness of corroded reinforced concrete structures. Ph.D. Thesis. Universidade Nova de Lisboa.

- Eyre, JR and Nokhasteh, MA. Strength assessment of corrosion damaged reinforced

concrete slabs and beams. Proceedings of the ICE-Structures and Buildings, 94(2):197–

203.

- Fink, Steiger and Kohler (2009). Definition of robustness and relative terms. Slovenia

- Frangopol D. M., CURLEY J. P. Effects of Damage and Redundancy on Structural Reliability. Journal of Structural Engineering, Vol. 113, No. 7, 1987, pp. 1533-1549.

- Ghosn and Moses (1998). Redundancy in Highway Bridge Substructures. Washington D.C.: National academy press.

- Hambly, 1991, Bridge deck behaviour, Spon edition, London

- Hernnikoff, A. 1941. Solution of problems of elasticity by the Framework Method, Journal of Applied Mechanics, December.

- John P.Miller (2012). Fundamental of post tensioned concrete design for buildings. : SunCam

- Lind, NC. A measure of vulnerability and damage tolerance. Reliability engineering &

systems safety, 48(1):1–6, 1995.

- Nawy, E G (1996). Prestressed concrete. A fundamental approach. 2nd ed. Upper Saddle River: Prentice Hall, Incorporated.

- Post tensioning institute. (December 2000). What is post-tensioning? Post tensioning journal. pages 1 and 2

- Starossek U., Haberland, M. Approaches to measures of structural robustness, Structure and Infrastructure Engineering, Vol. 7, No. 7-8, 2011, pp. 625-631.

- Thoft-Christensen, Palle; Sørensen, John Dalsgaard; Hansen, H. I. Proceedings from Symposium on Risk Analysis, Ann Arbor, USA, August 11-12, 1994. 1994. p. 239-248.

- VSL Report series (1991). Detailing for post-tensioned. Bern, Switzerland: VSL INTERNATIONAL LTD.

- VSL Report series (1991), Post tensioned slab. Bern, Switzerland: VSL INTERNATIONAL LTD.